



Tomas Bata University in Zlín

Centre of Polymer Systems

Doctoral Thesis Summary

Chemical Modification of Polysaccharides for Biomedical Applications

Chemická modifikace polysacharidů pro biomedicínské aplikace

Author: Ing. Kateřina Štěpánková, Ph.D.

Degree programme: P3924 Materials Science and Engineering

Degree course: 3911V040 Biomaterials and Biocomposites

Supervisor: Assoc. Prof. Marián Lehocký, Ph.D.

Consultant: MSc. Kadir Ozaltin, Ph.D.

Reviewers: prof. RNDr. František Krčma, Ph.D.
prof. Ing. et Ing. Ivo Kuřitka, Ph.D. et Ph.D.

Zlín, February 2024

© Kateřina Štěpánková

Published by **Tomas Bata University in Zlín** in the Edition **Doctoral Thesis Summary**.

The publication was issued in the year 2024

Key words in Czech: *chemická modifikace, furcellaran, hemokompatibilita, biokompatibilita, povrchové povlaky, biomateriály*

Key words: *chemical modification, furcellaran, hemocompatibility, biocompatibility, surface coatings, biomaterials*

Full text of the doctoral thesis is available in the Library of TBU in Zlín.

ISBN 978-80-7678-240-2

ACKNOWLEDGEMENT

I would like to convey my sincere gratitude to my supervisor, doc. Assoc. Prof. Marian Lehocký, Ph.D. for providing invaluable feedback, imparting knowledge and sharing his expertise with me. I would also like to extend my thanks to my consultant MSc. Kadir Ozaltin, Ph.D. for his guidance and encouragement throughout my work.

I am grateful to my colleagues and friends at the Centre of Polymer Systems for their assistance, advice, and companionship during my studies.

My special thanks are devoted to Monika Muchová for being my soulmate, emotional support and well of patience during the challenging times. I would like to thank Alžběta Důbravová for endless positivity and enthusiasm and Ilkay Karakurt for being a constant source of inspiration throughout my research journey.

Last but not least, I cannot forget to acknowledge my wonderful parents for their unwavering motivation, their constant encouragement, invaluable support and never losing a hope in me.

This work was supported by internal grants of TBU in Zlín project no. IGA/CPS/2019/001, IGA/CPS/2020/001, IGA/CPS/2021/001, IGA/CPS/2022/001 and IGA/CPS /2023/001.

ABSTRACT

The objective of the present study was to explore the potential of furcellaran in biomedical applications. Furcellaran was immobilized onto polyethylene terephthalate (PET) surfaces via a multistep process, and the resultant surfaces were characterized by relevant analytical techniques. The immobilized furcellaran was then tested to antibacterial and anticoagulant properties, as well as cytocompatibility with fibroblasts and stem cells. The findings suggest that PET films coated with furcellaran exhibited a significant increase in the proliferation of embryonic stem cells (ESCs) when compared to the untreated material. Furcellaran was also sulfated using four different methods to improve its hemocompatibility, and the resulting sulfates were confirmed by FT-IR and XPS. The study found that the introduction of sulfate esters into furcellaran increased its anticoagulant activity while the furcellaran prepared via chlorosulfonic acid had the highest effect on the coagulation cascade. All tested samples were non-cytotoxic up to the concentration of 0.1 mg/mL. Sulfated derivatives immobilized on the PET surface via radiofrequency plasma exhibited a reduction in adhesion and aggregation of platelets and inactivation of all their stages.

Keywords: chemical modification, furcellaran, hemocompatibility, biocompatibility, coatings, biomaterials

ABSTRACT

Cílem této studie bylo prozkoumat potenciál furcellaranu v biomedicínských aplikacích. Furcellaran byl imobilizován na povrchy polyethylentereftalátu (PET) pomocí vícekrokového procesu a výsledné povrchy byly charakterizovány pomocí relevantních analytických metod. Imobilizovaný furcellaran byl poté podroben testům antibakteriální a antikoagulační účinnosti a testům s fibroblasty a kmenovými buňkami. Výsledky naznačují, že PET filmy potažené furcellaranem vykazovaly významný nárůst proliferace embryonálních kmenových buněk (ESCs) v porovnání s neupraveným polymerem. Furcellaran byl také sulfatován čtyřmi různými metodami s cílem zlepšit jeho hemokompatibilitu, kde výsledné sulfáty byly potvrzeny pomocí FT-IR a XPS. Studie ukázala, že zavedení sulfátových esterů do struktury polysacharidu zvýšilo jeho antikoagulační aktivitu a furcellaran připravený pomocí chlorosulfonové kyseliny měl největší efekt na koagulační kaskádu. Všechny testované vzorky byly necytotoxické do koncentrace 0.1 mg/mL. Mimo jiné sulfatované deriváty imobilizované na PET povrchu pomocí radiofrekvenční plazmy vykazovaly redukci adheze a agregace krevních destiček a inaktivaci všech jejich stádií.

Klíčová slova: *chemická modifikace, furcellaran, hemokompatibilita, biokompatibilita, povlaky, biomateriály*

TABLE OF CONTENT

| | |
|--|----|
| ACKNOWLEDGEMENT | 3 |
| ABSTRACT | 4 |
| ABSTRACT | 5 |
| 1. INTRODUCTION | 8 |
| 2. BIOMATERIALS | 9 |
| 2.1 Non-degradable polymers | 9 |
| 2.2 Biodegradable polymers | 10 |
| 3. SURFACE FUNCTIONALIZATION | 11 |
| 3.1 Plasma Treatment..... | 11 |
| 4. BIOMOLECULE IMMOBILIZATION | 13 |
| 4.1 Bioactive surface for enhanced cell proliferation | 14 |
| 4.2 Bioactive surface for enhanced hemocompatibility..... | 15 |
| 5. SEAWEED POLYSACCHARIDES | 16 |
| 5.1 Furcellaran..... | 17 |
| 6. CHEMICAL MODIFICATION | 18 |
| 6.1 Sulfation | 18 |
| 7. IMMOBILIZATION APPROACHES | 20 |
| 7.1 Radical graft copolymerization..... | 20 |
| 7.2 Non-covalent physical adsorption..... | 21 |
| AIMS OF THE DOCTORAL THESIS | 23 |
| 8. EXPERIMENTAL PART | 24 |
| 8.1 Deposition of native furcellaran onto PET films | 24 |
| 8.1.1 Preparation | 24 |
| 8.1.2 Characterization of films..... | 25 |
| 8.1.3 Evaluation of biological activity | 25 |

| | | |
|---|--|-----------|
| 8.1.4 | Results and Discussion | 25 |
| 8.1.5 | Conclusion | 32 |
| 8.2 | Chemical modification of furcellaran for enhanced blood compatibility..... | 33 |
| 8.2.1 | Preparation | 34 |
| 8.2.2 | Characterization of sulfated derivates..... | 35 |
| 8.2.3 | Evaluation of hemocompatibility..... | 35 |
| 8.2.4 | Results and Discussion | 35 |
| 8.2.5 | Conclusion | 42 |
| SUMMARY OF WORK AND CONTRIBUTION TO SCIENCE..... | | 44 |
| LIST OF FIGURES | | 56 |
| LIST OF PUBLICATIONS..... | | 59 |
| CURRICULUM VITAE..... | | 61 |
| CONFERENCES ATTENDED..... | | 63 |

1. INTRODUCTION

Over the past twenty years, numerous studies have been carried out to explore the potential biomedical applications of polysaccharides derived from seaweed¹. These polysaccharides have properties such as hydrogel formation under certain pH conditions, biocompatibility, and non-toxicity, which make them an attractive option for use in various biomedical fields, including drug delivery and tissue engineering². The field of polysaccharide biotechnology is rapidly expanding, and seaweed is known to contain a wide range of biologically active compounds that have functional applications in areas such as functional foods and pharmaceuticals, as well as tissue engineering³.

There are various ways to explore the potential of marine algae polysaccharides for biomedical applications. One approach is to modify the existing polysaccharides chemically by incorporating functional groups that impart desirable properties. The modification can be achieved either by attaching functional moieties or by directly altering the repeating unit of the saccharides. Another way is to expand the current range of hydrogel-forming polysaccharides extracted from seaweed, which can open up new avenues of applications. This can be done by developing advanced methods for extraction and identifying new seaweed species that may contain previously undiscovered polysaccharides⁴.

Seaweed polysaccharides can adhere to surfaces and create coatings, which makes them useful for immobilizing on polymer surfaces. This can improve the interactions with target tissues or enable the release of drugs in response to environmental cues⁵.

The presented thesis is therefore devoted to investigation of biological effects of furcellaran by the preparation of bioactive surfaces and subsequent chemical modification.

In the first section a general overview of biomaterials, surface functionalization, immobilization approaches and chemical modification are reported. At the end a general introduction to furcellaran, chemical modification and motives for use this polysaccharide in biomedical applications are given. In second section, the experimental part, the method used for furcellaran preparation and characterization, biological assays and the most significant results are illustrated.

2. BIOMATERIALS

Biomaterials have been instrumental in transforming medicine over the last few decades. These refer to both naturally-occurring and synthetic materials, such as polymeric materials, metals, ceramic materials, and their composites, that can be seamlessly integrated into the human body without causing harm to living tissues due to their biocompatibility⁶.

Biomaterials must be biocompatible meaning that they perform their function with an appropriate host response. Throughout history, there have been three distinguishable groups of biomaterials categorized as "bioinert", "biocompatible", and "bioactive," based on their level their interactions with the body⁷.

Another attractive category of innovative materials that are advancing novel medical approaches are the ones taking the name of "smart biomaterials". These biomaterials have the capacity to change their physical, chemical, and mechanical characteristics in response to a variety of signals such as temperature, humidity, pH, redox potential, enzymatic activity, light, and mechanical stimuli⁸. Among illustrative examples of smart polymers are hydrogels using reversible techniques for crosslinking like physical cross-linking, thermally induced entanglement, and self-assembly, which may regulate the rate of drug release and biodegradation⁹.

According to the European Society for Biomaterials Consensus Conference-II, biomaterial is defined as "*the material anticipated interfacing in our biological systems in order to estimate the augment, treat or replacement of any tissue, organ or the functioning of the body*"¹⁰.

2.1 Non-degradable polymers

Nondegradable polymers have been widely used in the biomedical field for various applications such as drug delivery, implantable devices, tissue engineering scaffolds, fillings, ophthalmic lenses, heart valves, bone cement etc.¹¹

These group of polymers can have advantage of offering enduring support over time along with the ultimate performance during the patient's lifetime¹². It can also prevent complications arising from asynchronous degradation with new tissue regeneration and potentially harmful by-products of degraded polymers¹¹. The main categories of non-degradable synthetic polymers utilized in various biomedical applications include poly(urethanes), poly(carbonates), poly(siloxanes) and poly(sulphones)¹³.

While non-degradable polymers may provide long-term benefits, their biostability is also an important consideration that should be addressed to ensure their safety¹⁴.

However, there are existing disadvantages associated with the use of non-degradable polymers, including the risk of destructive inflammation and development of biomaterial-associated infection (BAI)¹⁵. Bacteria attach to biomaterial surfaces or

surrounding tissue via adhesion molecules which target a vast array of absorbed proteins and surface chemistries. Upon adhesion, the bacteria undergo a change in phenotype, resulting in the formation of a biofilm. In this mode of growth exhibit an increased resistance to antimicrobial treatments that has been attributed to the compromising of the immune system leading to foreign body reaction¹⁵.

Surface functionalization of non-degradable polymers has been used to improve polymer-cell interaction, prevent undesirable bacterial adhesion and avoid biomaterial induced blood thrombosis. Beside its bulk material advantages, availability of creating bioactive surfaces can provide significantly improved cytocompatibility.

2.2 Biodegradable polymers

Nondegradable polymers have been widely used in the biomedical field for various applications such as drug delivery, implantable devices, tissue engineering scaffolds, fillings, ophthalmic lenses, heart valves, bone cement etc.

The use of biodegradable polymers has revolutionized medical treatment in a highly innovative manner, primarily due to their excellent biocompatibility and biodegradability. The materials are designed to function for a limited time before the controlled degradation process, resulting in readily discarded products¹⁶.

Biodegradable polymers can be roughly categorized into two main classes – natural and synthetic – based on their source, composition, synthesis method potential application and economic importance¹⁷.

Natural polymers include proteins, polysaccharides, nucleic acids, lipids and native polyesters– polyhydroxyalkanoates (PHA)¹⁸. These materials exhibit highly varied characteristics that depend on the conditions under which they are employed and possess several advantages such cell function and adhesion support, susceptibility to cell-triggered proteolytic degradation and natural remodeling¹⁹. On the other hand, controlling the mechanical properties and degradation rates is challenging. Furthermore, there are the existing tendency for natural polymer to elicit antigenicity and higher susceptibility to infections²⁰.

Synthetic BPMs (biodegradable polymer materials) are manufactured by conventional polymerization procedure and are primarily made from natural resources and oil, respectively. There can be distinguished two classes of synthetic BPMs: bio-based polymers such as PLA, and oil-based monomer like PCL²¹.

While the degradation time of biodegradable polymers in the body may differ, it is crucial for the biomaterial to degrade at a pace that aligns with the regeneration and healing process to ensure proper remodeling of the tissue²². Moreover, the biomaterial must possess adequate permeability and processability for designed application^{18,22}.

In contrast to natural BPMs, synthetic BPMs are generally biologically inert and can be tailored to gain greater range of chemical and mechanical properties²³.

Although synthetic BPMs can prevent complications related to immunogenicity. Thus, significant research is being conducted on synthetic BPMs in order to avoid long-term effects associated with non-degradable polymers, such as scarring and inflammation²⁴.

3. SURFACE FUNCTIONALIZATION

Since cell-biomaterial interactions primarily occur at the interface, specific features of the biomaterial's surface such as roughness, hydrophilicity, chemistry, free energy and morphology play a significant role in determining the success of the implant²⁵. To enhance the cell-biomaterial interactions, it is necessary to optimize its physical, chemical, and biological properties.

Surface modification can be categorized into two types: physical and chemical. Physical modification alters the surface's topography or morphology while leaving the chemistry largely unchanged, through techniques like etching, grit blasting, and machining. On the other hand, chemical modification techniques involve the use of methods like cold plasma and chemical vapor deposition, atomic layer deposition, and electro-chemical deposition, all of which have well-established applications²⁶. Unlike physical treatment, this method is permanent, as the modification creates stable covalent bond between biomolecules and the polymer surface. One advantage of chemical treatment is that it creates stable bioactive sites on the surface, allowing for the immobilization of additional biomolecules and improving the biological properties of the surface. This facilitates favorable attachment and growth of cells on the surface. However, there is a potential risk that uncontrolled chemical functionalization in the preactivated state may alter the bulk properties of the polymeric material²⁷.

Several surface functionalizing approaches have been employed to enhance the performance of biomaterials, particularly at the interface of the material such as wet chemistry, plasma treatment, surface graft polymerization and biomolecule immobilization.

3.1 Plasma Treatment

The process for plasma generation requires the application of energy on gas, which causes its ionization. Plasma can be categorized into two groups, either non-thermal (cold) and thermal (hot) plasma (Figure 1), depending on the temperature of its electrons, along with factors such as the level of ionization, atmospheric pressure, and prevailing temperature conditions. Thermal plasmas are in equilibrium state, whereby the temperature of all particles, including electrons, ions and gas is uniform. In contrast, plasmas that exhibit significant deviations from kinetic equilibrium have electron temperatures higher ($\approx 10,000$ K) than the temperature of the ions and neutrals (≈ 300 – 1000 K) and are classified as nonequilibrium (non-thermal) plasmas^{28,29}.

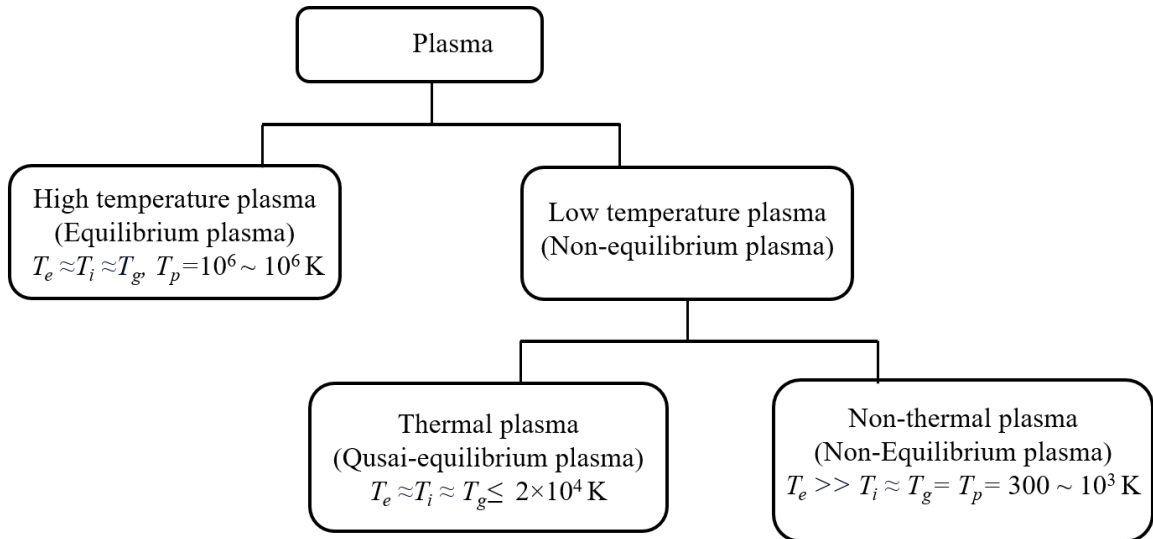


Figure 1 Plasma classification. Note: T_e = electron temperature, T_i = ion temperature, T_g = gas temperature³⁰

The damaging effects of high temperatures on polymers are well-known, and thermal plasmas with high temperatures are not suitable for polymer surface modification. Consequently, most applications involving the modification of polymer surfaces typically rely on nonthermal or cold plasmas²⁸.

Cold plasmas are gases that are only slightly ionized and can be generated either at low or atmospheric pressures (Figure 2).

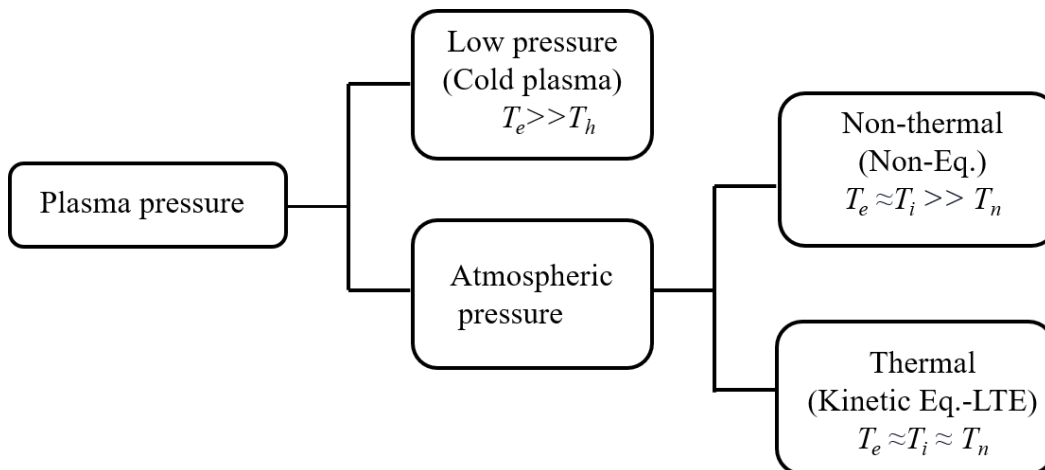


Figure 2 Plasma classification based on pressure³⁰

Atmospheric pressure plasmas are plasmas that can be created by subjecting a gas to high electrical fields under normal atmospheric pressure. There are various methods to achieve this, such as corona discharge, arc discharge, dielectric barrier discharge (DBD), atmospheric pressure glow discharge (APGD), and plasma jets. One of the

significant benefits of atmospheric pressure plasmas is their easy and relatively inexpensive production. Unlike low-pressure plasmas, they don't require vacuum components, which makes them more accessible and compatible with various applications. Low pressure plasmas are generated in a vacuum chamber, with an applied voltage between the anode and cathode of a few hundred volts having electrons with energies between 1 to 10 (eV), and a low level of ionization ranging from 10^{-6} to 10^{-3} ^{31,32}. They are typically excited and maintained using various electrical methods, such as applying radio frequency (RF) power, microwave (MW) power, alternating current (AC), or direct current (DC)^{29,33}. To create a dc discharge, two conductive electrodes are placed in a low-pressure gas-filled chamber. AC (alternating current) plasma encompass both radio frequency (RF) and microwave (MW) plasmas, which are generated by higher frequencies (13.56 MHz and 2.45 GHz, respectively)³⁴.

In literature, plasma treatment is commonly classified as a physical hydrophilic functionalization method³⁵. However, plasma treatment causes notable chemical changes on the polymer surface, including the breakage of chemical bonds. This leads to the introduction of various functional groups and reactive radicals³⁶. The functionalization process is primarily controlled by the main parameters: the type of plasma source, duration of treatment, carrier gas and its flow rate, applied voltage, frequency that creates different plasma type, electron density and plasma energy. To enhance biocompatibility and enable the covalent immobilization of different bioactive molecules, it is essential to use an appropriate plasma source that can effectively target the surface³⁷.

Plasma treatment offers several benefits, such as being environmentally friendly and not altering the bulk or mechanical properties of polymers³⁸. There are also existing limitations, including to inability to uniformly modify the entire surface of polymers and also the hydrophilic effect is not permanent.³⁹ To prolong the effectiveness of plasma treatment and prevent surface restructuring, it is recommended to perform post-plasma grafting of allylamine and other monomers⁴⁰.

4. BIOMOLECULE IMMOBILIZATION

Physical/chemical functionalization confers the advantageous provision of stable bioactive sites, facilitating subsequent immobilization of biomolecules, thereby culminating in the enhancement of a polymer surface biological characteristics to drive its cellular interactions for the specific site in which its application is intended. The concept of using biomolecules like proteins, peptides, ligands, receptors, lipids, carbohydrates etc., is gaining great attention due to their nontoxic nature, biocompatibility, mimicking property and ability to mitigate unfavorable reactions, such as inflammation and platelet adhesion, often triggered by synthetic polymer surfaces²⁸. Furthermore, biofunctionalization will promote cell adhesion,

proliferation, and differentiation, thereby offering substantial potential for tissue regeneration and wound healing applications⁴¹. Biomolecules are applied onto material surface through innovative mechanisms and the prerequisites in terms of surface chemistry and morphology vary for different biomedical applications and entirely contrasting requirements may arise for the same material⁴².

4.1 Bioactive surface for enhanced cell proliferation

Recent developments in biomaterials for tissue engineering have shifted their focus towards the creation of biomimetic materials designed to induce precise cellular responses and facilitate new tissue formation through biomolecular recognition. Biomolecular recognition is achieved by surface and bulk modifications of biomaterials through chemical or physical means. Utilizing bioactive molecules, including native extracellular matrix (ECM) proteins and derived short peptide sequences, fosters specific interactions with cell receptors⁴³. Consequently, protein-coated biomimetic materials can mimic numerous ECM functions in living tissues⁴⁴. Cell adhesion and proliferation are significantly dependent on the protein absorption onto the polymeric biomaterial via integrin receptors that govern cell adhesion interactions⁴⁵. Hence, the controlled modulation of surface-protein interactions is crucial for promoting cell proliferation. In contrast, uncontrolled interactions often result in negative effects such as platelet activation, the release of coagulation factors, initiation of the complement cascade, inflammation, and microbial attachment⁴⁶.

In clinical tissue engineering, fibroblast cells (Figure 3-A)), which are typically located in connective tissues, play a crucial role in the process of healing wounds and regenerating damaged tissue⁴⁷. Embryonic stem cells (ESCs) (Figure 3-B)) are derived form of the blastocyst inner cell mass and are particularly favored for studies related to cell proliferation. This preference arises from their pluripotency and self-renewing ability, which signifies their capacity to differentiate into a wide range of cell lineages in living bodies while maintaining an undifferentiated state during *in vitro* culture⁴⁸.

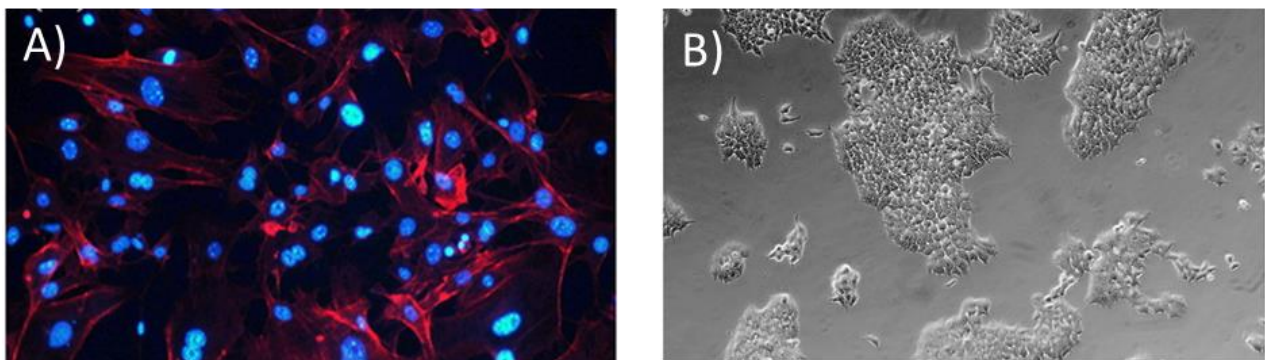


Figure 3 Morphology of A) fibroblasts NIH/3T3 and B) embryonic stem cells ES R1 line^{47,49}

4.2 Bioactive surface for enhanced hemocompatibility

Blood-contacting biomaterials intended for implantation or tissue replacement must prevent surface induced blood coagulation, thrombus formation and complement activation. The contact of synthetic biomaterial with blood immediately leads to reversible or irreversible protein adsorption in accordance with Vroman effect⁵⁰. The final adsorbed layer comprises a diverse array of proteins, encompassing fibrinogen, various coagulation factors, immunoglobulins, and adhesive proteins such as fibronectin and vitronectin⁵¹. The existence of the adsorption layer can be linked to the activation of both the blood coagulation and complement systems, as well as the adhesion and activation of blood platelets and leukocytes⁴⁶.

In general, negatively-charged surfaces tend to result in less protein adsorption compared to positively-charged surfaces. This is because, at physiological pH values, many proteins carry a net negative charge, creating a repulsive force⁵². Positively-charged surfaces notably enhance protein adsorption and can potentially induce conformational changes of proteins. Even when there are protein domains with opposite charges, resulting in an overall repulsive Coulomb force against the surface, protein adsorption can still occur due to attractive forces between these oppositely charged protein domains and the surface⁵².

The intrinsic pathway, referred to as contact activation of coagulation cascade, has greater significance concerning blood-contacting devices. This pathway is initiated when Hageman factor and HMWK adsorb onto negatively-charged surfaces⁵³. As the presence of negative charges prevents protein adsorption, it can also cause an increase in contact system activation if the charge density is too high, it is imperative that the charge density on a material surface is carefully tuned by adding positively charged groups that increase their zeta potential⁵⁴.

The extrinsic pathway is initiated in response to vascular injury when cells containing tissue factor (TF) come into contact with blood. TF is found within the ECM beneath endothelial cells, as well as in fibroblasts and smooth muscle cells⁵⁵. It has become evident that contact between blood and artificial materials can potentially activate the extrinsic pathway due to TF expression by monocytes⁵⁶. Both the extrinsic and intrinsic pathways lead to the activation of FX to form FXa, which serves as the initial stage of the common pathway. FXa, in conjunction with activated cofactor V (FVa), catalyzes the conversion of prothrombin into thrombin. Subsequently, thrombin participates in the polymerization of fibrinogen, transforming it into fibrin⁵⁷.

Low-molecular-weight heparin (LMWH) is currently utilized in clinical practice for preventing thromboembolic disorders. However, its disadvantages such as the risk of thrombocytopenia and the risk of contamination necessitate the exploration of alternative options⁵⁸. Recently, there has been a focus on seaweed polysaccharides due to their abundant marine storage and biocompatibility⁵⁹.

Adsorbed plasma proteins, particularly fibrinogen, induce platelet adhesion and activation on foreign surfaces. When platelets adhere to biomaterial surfaces, it serves as an indication of the material's tendency to promote blood clot formation and coagulation activation. It has been demonstrated that platelet adhesion, spreading, and aggregation are increased on hydrophobic polymer membranes but reduced on hydrophilic surfaces⁶⁰.

Platelets circulate in the bloodstream in a disk-shape form, and after a contact with a foreign surface, they undergo a sequence of activation steps that result in alterations to their shape (Figure 4). These changes in adhered platelets involve the extension of pseudopodia and the spreading of the hyalomeres across the surface of the foreign body. The morphology of the adhered platelets offers a way to describe the activation changes of platelets.

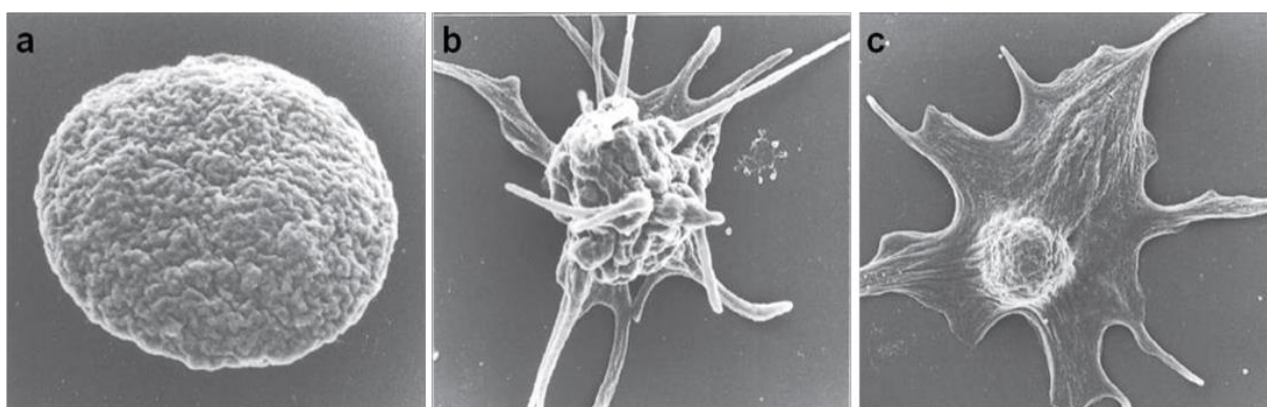


Figure 4 Discoid platelet (a), dendritic platelet (b) and spread platelet (c) photographed in the low-voltage, high-resolution SEM⁶¹

5. SEAWEED POLYSACCHARIDES

Marine-derived polysaccharides have gained significant importance because of their remarkable therapeutic characteristics, leading to their utilization in tissue engineering, coating for stents, and immobilizing biomolecules, adding substantial value to these applications⁶². Numerous sulfated polysaccharides have been employed as antiviral agents against viruses such as respiratory syncytial virus (RSV), herpes simplex virus (HSV) types 1 and 2, and human immunodeficiency virus (HIV)⁶³. Carrageenan, in particular, has shown promise in laboratory settings as a potential agent for conferring antiviral effects, including HIV prevention and addressing other sexually transmitted diseases⁶³. Fucoidan has been applied as a coating on stent surfaces to inhibit restenosis, a process driven by the proliferation of smooth muscle cells (SMC) over the stent⁶⁴. Ulvan/chitosan hydrogel facilitated the attachment and proliferation of osteoblasts, indicating their potential as valuable platforms for promoting bone tissue regeneration⁶⁵.

5.1 Furcellaran

Furcellaran, a sulfated anionic galactan, is extracted from the red algae *Furcellaria lumbricalis*, which is found in the North Atlantic and brackish waters of the Baltic sea. Loose-lying *F. lumbricalis* is particularly abundant in Estonia and is believed to have the highest concentration in the world.⁶⁶ The floating mass of seaweed can be harvested for commercial purposes, and since the 1960s, the phycocolloid industry in the area has been utilizing it specifically for the production of furcellaran⁶⁶. Each year, the total amount of biomass fluctuates, but it typically falls between 100,000 and 200,000 tons based on wet weight. The majority, ranging from 60% to 73%, is attributed to *F. lumbricalis*⁶⁷.

Furcellaran is chemically and functionally comparable to κ -carrageenan (Figure 5), however the quantity of sulfate esters in furcellaran is different. It consists of repeating backbone of alternating (1 \rightarrow 4)-3,6-anhydro- α -D-galactopyranose-(1 \rightarrow 3)- β -D-galactopyranose-4'-sulfate (28.5–30.1%), 1,3-linked galactose (20%), 1,4-linked galactose (8%) and 1,4-linked 3-O-methyl-galactose (2%) structural units with approximately one sulfate ester per three monomer residues⁶⁸. The reported weight-average molar mass values for furcellaran in literature differ, ranging from approximately 290 to 500 kDa, depending on the method of extraction used⁶⁸.

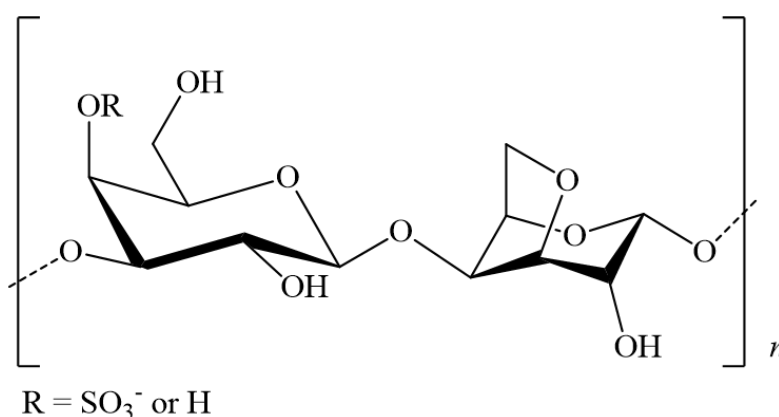


Figure 5 *Furcellaran structure*

F. lumbricalis has distinct chemical characteristics, with a relatively high concentration of protein pigments that makes it rich in nitrogen compared to other species of red algae. Typically, the nitrogen content in *F. lumbricalis* varies from 1.1% to 4.8% of its dry mass⁶⁹. Furcellaran is commonly extracted using water or alkaline solutions. Algae is washed and treated with a selected alkali to extract the polysaccharide, which forms stronger chains after prolonged treatment. The choice of alkali affects dispersion, hydration, thickening, and gel formation⁷⁰.

Furcellaran's key characteristic is its capacity to form a gel, which relies not only on factors such as polysaccharide structure, concentration, and temperature, but also on the presence of co- and counter-ions such as K^+ , Na^+ , Mg^+ and Ca^{+71} . The resulting helices then aggregate in a cation-specific manner, leading to the formation of a gel⁶⁹. For this reason, furcellaran is currently applied as a gelling-stabilizing agent in food processing⁷², as a component for the development of edible films and coatings⁷³ as well as multilayer capsules for drug delivery⁷⁴. Recently, it has been proposed as biopolymer matrix enriched with polysaccharides with antioxidant properties and improved physic-chemical traits⁷⁵. In conjunction with carrageenan is also classified for use as food additives under European Union legislation⁷⁰.

6. CHEMICAL MODIFICATION

The significance and relevance of biomaterials derived from sulfated polysaccharides as biotech pharmaceuticals can be attributed to two key factors. Firstly, their glycosidic bonds are susceptible to enzymatic cleavage, facilitating biodegradability. Secondly, the inclusion of negatively charged sulfate groups enhances their polyelectrolyte properties and allows for tailoring to specific applications through functionalization⁷⁶, apart from a privileged interaction with negatively charged epithelia. Moreover, the existence of hydroxyl groups (OH) within these polymers offers essential components for various chemical alterations. This includes the incorporation of hydrophobic, acidic, or alkaline groups, as well as other functionalities into the polysaccharide structures. Such modifications have the potential to modify the characteristics of biopolymers, allowing for targeted customization to achieve specific goals⁷⁷. Currently, the established molecular modification techniques for polysaccharides encompass carboxymethylation, phosphorylation, sulfonation, sulfation, methylation, selenization and alkylation. These methods have substantially improved the water solubility of original polysaccharides and even introduced new bioactive features⁷⁸.

6.1 Sulfation

The sulfate group is a ubiquitous post-translational modification that contributes to several biological processes, including protein-protein interactions. It makes up around 1% of all known epigenetic markers⁷⁹. Particular attention is directed to sulfated polysaccharides, specifically, glycosaminoglycans (GAGs).

In the last twenty years, there has been a growing interest in using plant polysaccharides as an alternative, sustainable source of GAGs analogs. Only a few plant species have sulfated polysaccharides, and they are all found in salty environments, further supporting their marine origin and probable function in salt tolerance⁸⁰. Seaweed polysaccharides like sulfated fucans or galactans are so far the

most studied representatives and an attractive alternative due to their abundant marine storage, biodegradability and biocompatibility⁸¹.

By chemically sulfating natural sulfated polysaccharides, it is possible to create oversulfated derivatives that have considerably different physical and biological properties from its precursor polysaccharide. Sulfates are formed by nucleophilic substitution of hydroxyl groups in polysaccharides⁸².

Methods for regioselective sulfation have been developed in order to create polysaccharides with predetermined patterns of sulfate groups. Recent findings suggest that in addition to the density of negative charges and its regiochemistry in polysaccharide backbone, several structural, also the arrangement of glycoside linkages, molecular weight, may also impact the potential bioactivity^{83,84}.

One approach for sulfation of polysaccharides involves the use of sulfuric acid as the sulfating agent along with dicyclohexylcarbodiimide (DCC) as a condensation reagent in dimethylformamide (Figure 6).

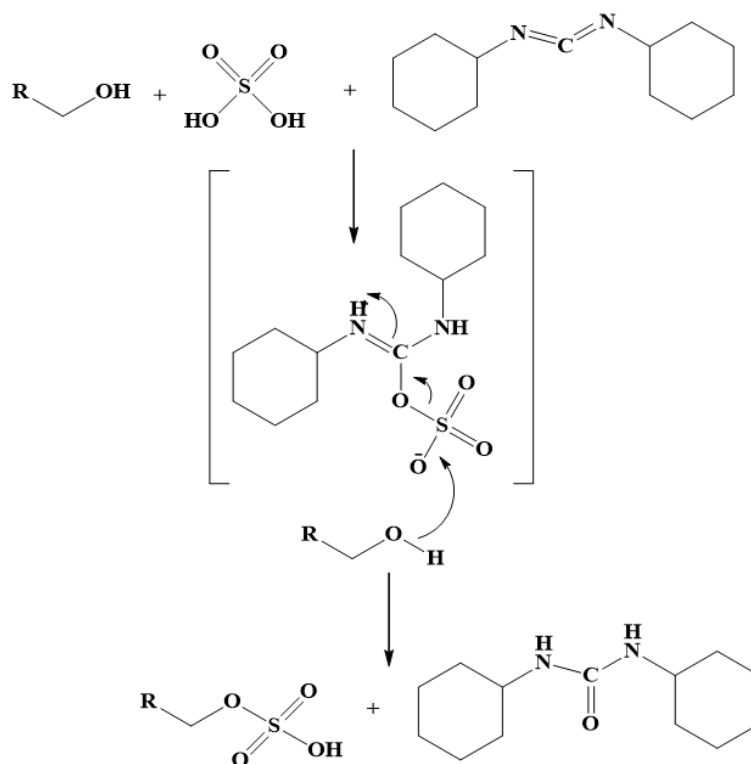


Figure 6 The proposed mechanism involves the formation of a solvated, protonated DCC/H₂SO₄ intermediate with a subsequent attack of the alcohol group on the sulfur atom, resulting in the production of dicyclohexylurea and the monosulfate ester⁸⁵

Due to sulfuric acid's potent acidity, it is impractical to sulfate using DCC/H₂SO₄ for a number of fragile structures. On the other hand, SO₃-amine based complexes provide better reaction regulation of reaction kinetics and enable milder sulfating conditions at lower to intermediate DS values⁸⁶. Although some cleavage of

glycosidic linkages and other acid labile functions are still accompanied, the incorporation of an protective groups, such as 2-methyl-2-butene was stated for non-degradative sulfation⁸⁷.

The chlorosulfonic acid-pyridine method is still the most commonly used approach for preparing sulfated polysaccharides due to the high DS values and yields that can be achieved using this method. Other reagents can be used as catalysts such as DMF (Figure 7) or 4-dimethylaminopyridine (DMAP)⁸⁸.

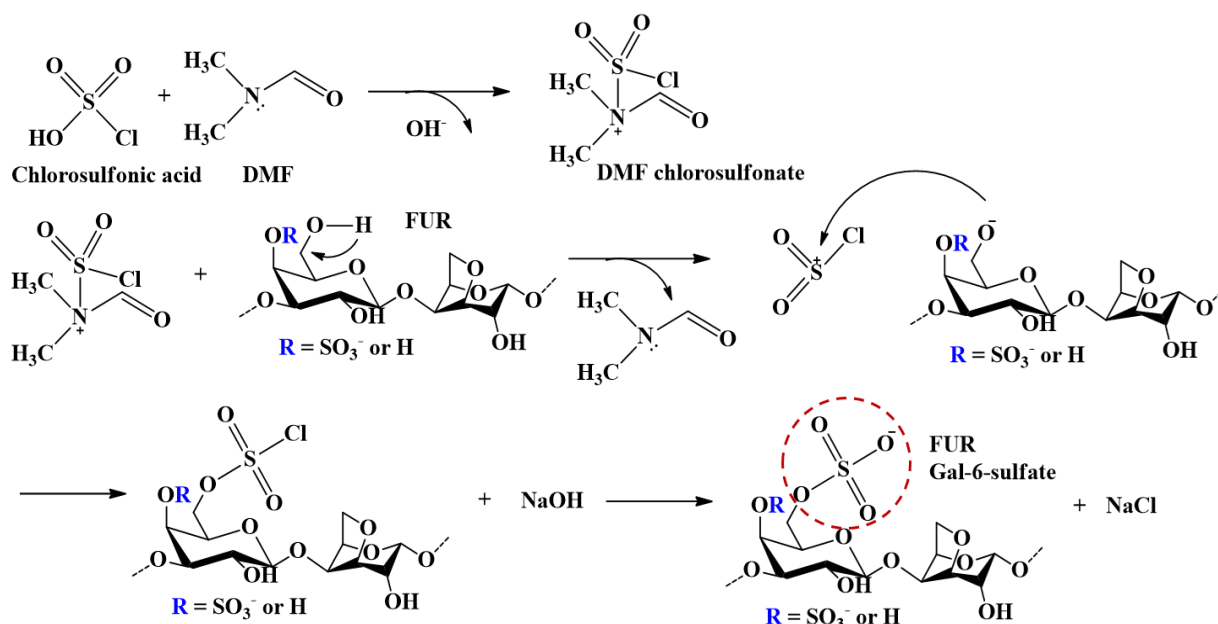


Figure 7 The suggested reaction mechanism furcellaran sulfation with chlorosulfonic acid and a dimethylformamide intermediate⁸⁹

7. IMMOBILIZATION APPROACHES

7.1 Radical graft copolymerization

Graft copolymerization is process that involves polymerizing a desired monomer onto the surface of a plasma-treated polymer, resulting in the creation of a grafted brush layer on top of the surface. Polymer brushes are essentially thin polymer films in which the individual monomer chains are attached to a solid interface through one end of the chain⁹⁰. This method is highly selective to the surface and only modifies the top few nanometers of the material, leaving the bulk properties unaffected⁹¹. The process of graft copolymerization involves the initiation of radical polymerization through free radicals and metastable species that form on the surface after plasma treatment. These active radicals are stable in vacuum but can react rapidly when exposed to a gas containing polymerizable molecules to create a polymer "brush-like"

structure on the surface. This type of structure is suitable for interacting with biomolecules through the creation of intramolecular forces⁹².

Huge diversity of precursors and monomers can be used for attaching biologically active molecules or compounds to various types of polymer surfaces, including gas mixtures to create amino groups⁹³. Due to presence of double bond, allylamine based monomers can be polymerized to create a long carbohydrate backbone with a high density of positively charged amine group side chains. The existence of unsaturated hydrocarbon implies that radicals react with other parts of the allylamine molecule that do not break the double bond. These reactions bring an end to the radicals and prevent further polymerization. The process of Beckman's rearrangement reaction may convert amine groups into oxime groups and nitrile groups via oxidation⁹⁴.

There are two main methods for preparing polymer brushes: physisorption and covalent attachment. Physisorption involves a reversible process in which polymer chains with sticking segments adsorb onto a suitable substrate. Process of covalent attachment can be achieved through the "grafting to" approach or the "grafting from" approach⁹⁵. The grafting methods include radical polymerization, ionic and ring-opening polymerization, and controlled/living radical polymerization⁹⁶.

7.2 Non-covalent physical adsorption

Of the various physical methods available, one effective and straightforward approach is the adsorption of polyelectrolytes onto charged surfaces through electrostatic interactions⁹⁷ (Figure 8). This type of physical adsorption is considered as method of hydrophilic and biological functionalization of polymer surface by spraying or soaking of polymer in biomolecule solution⁹⁸.

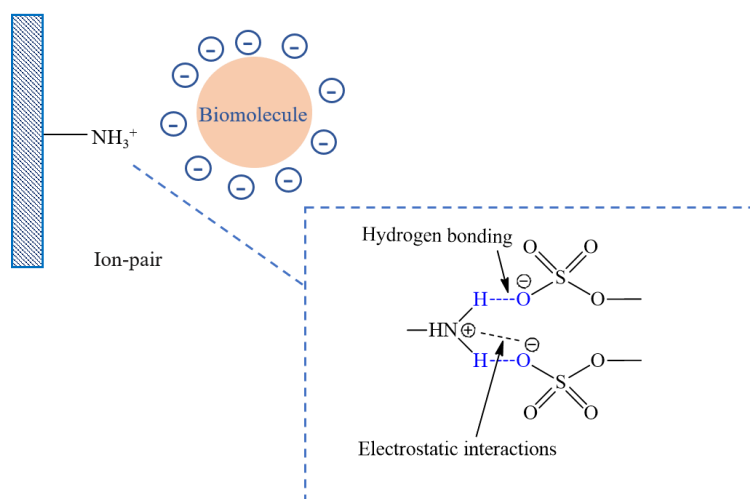


Figure 8 An adsorptive immobilization of biomolecule with sulfate group(s) and positively charged nitrogen containing groups on the surface by Coulomb-type interactions and hydrogen bonding

One major limitation of this immobilization approach is that the physical binding between the biomolecules and the surface of the polymer may not be permanent and can be easily removed by polar solvents or cell culture media. To overcome this limitation and improve cell affinity to the surface, it is necessary to combine this method with another surface functionalization method. Alternatively, chemical methods can be used to introduce active groups onto the surface of a material through straightforward chemical reactions such as hydrolysis or aminolysis⁹⁹. Pretreating the surface with ammonia plasma facilitates subsequent collagen adsorption through strong polar interactions and hydrogen bonds between the collagen and polar groups on the pretreated surface. Such modifications have been found to be more effective than simply soaking the samples in collagen solution for a few hours⁹⁸.

Although such modified surfaces can be useful, they can be unstable in situations where there are significant changes in the pH of the medium or the ionic strength. When immobilizing biomolecule using electrostatic force, the pH of the reaction solution and the isoelectric point of the biomolecule are important factors to consider. The biomolecule's surface can have either a positive or negative charge depending on how the pH of the solution compares to the biomolecule's isoelectric point (*pI*). This allows the biomolecule to be immobilized onto surfaces that have the opposite charge through ionic and highly polar interactions¹⁰⁰. This method is not reliant on toxic solvents, making it environmentally friendly and does not require strict control¹⁰¹.

AIMS OF THE DOCTORAL THESIS

The main objective of the study is to explore the potential use of furcellaran in biomedical applications and to enhance its bioactive properties through chemical modification.

The study will focus on the following key areas:

- Activation of polymer surface through radiofrequency plasma treatment and subsequent deposition of furcellaran onto the surface via grafting of polymeric brushes
- Characterization of the functionalized polymer surface and evaluation of its antibacterial activity, anticoagulant activity, cytotoxicity, and cell proliferation
- Chemical modification of furcellaran through various sulfation methods
- Assessment of the hemocompatibility of the sulfated derivatives

8. EXPERIMENTAL PART

8.1 Deposition of native furcellaran onto PET films

Sulfated seaweed polysaccharides have emerged as a possible alternative to animal-derived sulfated polysaccharides. While furcellaran and κ -carrageenan have structural similarities, they differ significantly in terms of molecular weight and sulfate concentration, which can affect their biological interactions. Furthermore, although being obtained from red seaweed, furcellaran and κ -carrageenan are derived from different species and might possess distinct biological properties. By performing biological experiments to characterize furcellaran, new options for its possible usage in biomedical applications can be explored, leading to the development of novel materials with distinct features and applications.

A comparative study was undertaken to evaluate the immobilization of furcellaran and κ -carrageenan onto PET surfaces utilizing a multistep technique in which N-allylmethylamine was grafted via air plasma treatment to achieve this goal. The functionalized films that resulted were tested for anticoagulant action, antibacterial activity, and cytocompatibility with fibroblasts and (EC) stem cells.

8.1.1 Preparation

To activate polymer surface, both sides of the PET films (BOBET foil; 100 μm) were subjected to low-pressure plasma for 60 s at a radio frequency of 13.56 MHz with discharge matching power was set to 50 W, and the applied air feed rate was 20 sccm under laboratory conditions (Figure 9).

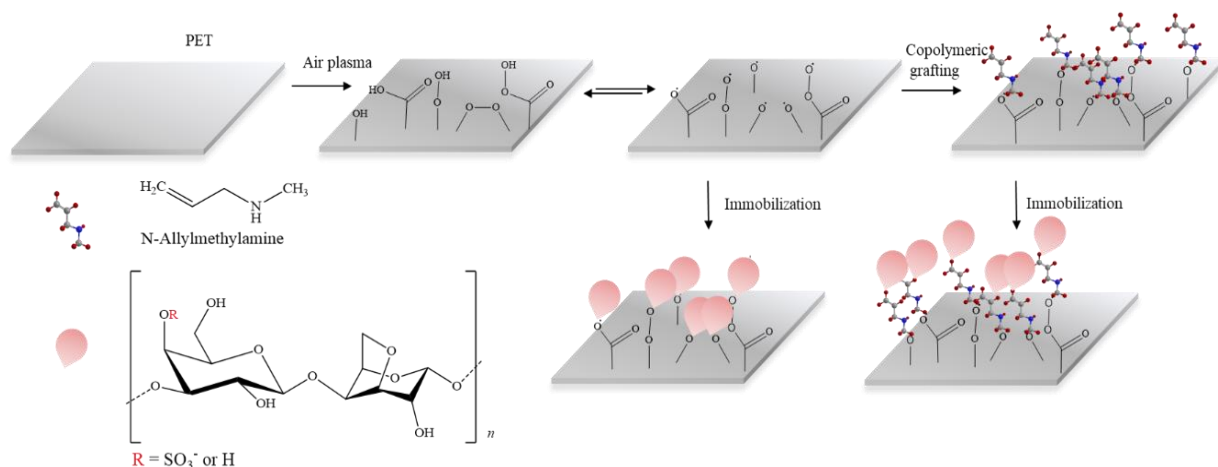


Figure 9 Schematic representation of plasma postirradiation grafting of N-allylmethylamine onto a PET surface followed by immobilization of FUR or κ -CA polysaccharide¹⁰².

The pressure inside the chamber was approximately 60 Pa. Some of the plasma-treated PET samples were then immediately exposed to saturated MAAM vapors to enable radical graft monomer polymerization towards polymer brushes for subsequent immobilization of tested polysaccharides. To compare, PET samples were also characterized and treated without MAAM grafting. Both, MAAM grafted and nongrafted PET samples were immersed into a 0.1% (w/v) solution of κ -CA and FUR for 24 h at room temperature for their immobilization onto a prepared polymer brush, followed by washing to remove any unbound polysaccharides and drying overnight at room temperature.

8.1.2 Characterization of films

Contact angle and surface energy, X-ray Photoelectron Spectroscopy (XPS), and Scanning Electron Microscopy (SEM) were used to characterize surface of prepared films. The detailed surface characterization of the samples is described in the relevant article, see¹⁰².

8.1.3 Evaluation of biological activity

The antibacterial activity was assessed using a modified version of the ISO 22196 standard. Anticoagulant activity testing was conducted in collaboration with KNTB hospital, and cell adhesion and proliferation were assessed in cooperation with Prof. Humpolíček research group at CPS, following ISO standard 10993 for the biological evaluation of medical devices. Details on the biological evaluation of prepared samples are outlined in the corresponding article, see¹⁰². Each of the samples was examined three times.

8.1.4 Results and Discussion

Surface chemistry and morphology

The contact angle values (Table 1) of the PET surface showed a substantial reduction after treatment with air plasma. This was attributed to the incorporation of oxidative functional groups onto the surface of the PET and tailoring of its morphology, leading to an increase in hydrophilicity and surface energy. These alterations rendered the PET surface more suitable for subsequent immobilization. The hydrophobicity of the immobilized FUR and κ -CA samples that were grafted onto polymer brushes exhibited an increase but remained less hydrophobic in comparison to the untreated PET surface. In contrast, no perceptible changes were observed in the films that lacked N-allylmethylamine (MAAM).

The initial PET foil demonstrated low surface energy values (γ_s) attributable to its low surface wettability. Nevertheless, following air plasma exposure, there was a significant increase in the γ_s value, which indicated a relatively substantial

surface polarity. Despite this modification, the discrepancies between the γ_s values of the plasma-treated PET and immobilized PET surfaces were insignificant.

Table 1 Contact angles (θ) (*w*: deionized water; *d*: diiodomethane; *f*: formamide) and surface free energy parameters of probe liquids used in the acid-base method (γ_s – total surface free energy, apolar γ_s^{LW} , polar γ_s^{AB} , Lewis acid γ_s^+ and base γ_s^- components)

| SAMPLE | Contact angles (°) for liquids | | | Surface free energy (mJ/m ²) | | | | |
|-----------|--------------------------------|------------|------------|--|-----------------|-----------------|--------------|--------------|
| | θ_w | θ_d | θ_f | γ_s | γ_s^{LW} | γ_s^{AB} | γ_s^+ | γ_s^- |
| PET | 63 ± 3 | 26.6 ± 0.5 | 54 ± 1 | 50.2 | 45.5 | 4.6 | 0.2 | 22.1 |
| PET_DC | 30 ± 3 | 25.6 ± 0.6 | 8.9 ± 1.2 | 57.6 | 45.9 | 11.7 | 0.8 | 38.8 |
| PET_MAAM | 33.7 ± 1.8 | 30.8 ± 0.4 | 12 ± 3 | 57.1 | 43.9 | 13.1 | 1.2 | 35.7 |
| MAAM_1000 | 40.9 ± 1.7 | 28 ± 3 | 18 ± 3 | 56.3 | 45.1 | 11.1 | 1.0 | 29.2 |
| MAAM_8500 | 47 ± 2 | 32 ± 2 | 20 ± 2 | 55.3 | 43.3 | 11.9 | 1.5 | 22.5 |
| MAAM_KAPA | 49 ± 2 | 28.2 ± 1.2 | 19 ± 2 | 56.1 | 44.9 | 11.1 | 1.5 | 20.0 |
| DC_1000 | 36.8 ± 1.4 | 18.1 ± 1.6 | 12 ± 2 | 57.9 | 48.3 | 9.6 | 0.7 | 32.6 |
| DC_8500 | 47 ± 2 | 21.7 ± 0.8 | 11.0 ± 1.5 | 58.3 | 47.2 | 11.0 | 1.4 | 20.6 |
| DC_KAPA | 46.7 ± 1.0 | 26.8 ± 1.9 | 11.3 ± 1.7 | 57.7 | 45.4 | 12.2 | 1.7 | 20.9 |

After analyzing the surface of untreated PET by XPS (Table 2), it was found to have 74.6% carbon and 25.4% oxygen. Plasma treatment led to an increase in oxygen content due to the incorporation of oxidized functional groups. Plasma treatment also resulted in a nitrogen content of 1.5%, with the highest nitrogen content observed in MAAM-grafted samples. However, the specimens that were not treated with MAAM had slightly higher oxygen levels. The presence of sulfur content in the MAAM_KAPA, DC_1000, DC_8500 and DC_KAPA samples indicates successful immobilization of polysaccharides, despite the relatively low levels of sulfur content. The sulfur and oxygen contents together support the effective immobilization of polysaccharides on the surface.

Table 2 Surface elemental composition (%)

| SAMPLE | C | N | O | S |
|-----------|------------|-----------|------------|-----|
| PET | 75 ± 2 | | 25.4 ± 1.1 | |
| PET_DC | 69 ± 2 | 1.5 ± 0.2 | 29.3 ± 1.2 | |
| PET_MAAM | 70 ± 3 | 2.1 ± 0.2 | 28.1 ± 1.2 | |
| MAAM_8500 | 74 ± 2 | 1.0 ± 0.2 | 25.3 ± 1.1 | |
| MAAM_1000 | 74.6 ± 1.3 | 1.0 ± 0.1 | 25 ± 2 | |
| MAAM_KAPA | 74 ± 2 | 0.9 ± 0.1 | 24.8 ± 1.3 | 0.2 |
| DC_1000 | 70 ± 2 | | 29.7 ± 2.1 | 0.3 |
| DC_8500 | 73.9 ± 1.1 | 0.6 ± 0.1 | 25.5 ± 1.4 | 0.1 |
| DC_KAPA | 73 ± 2 | 0.7 ± 0.1 | 26.5 ± 1.2 | 0.1 |

The outcomes of SEM are presented by micrographs in Figure 10, where the standard PET material displays homogenous and smooth morphology.

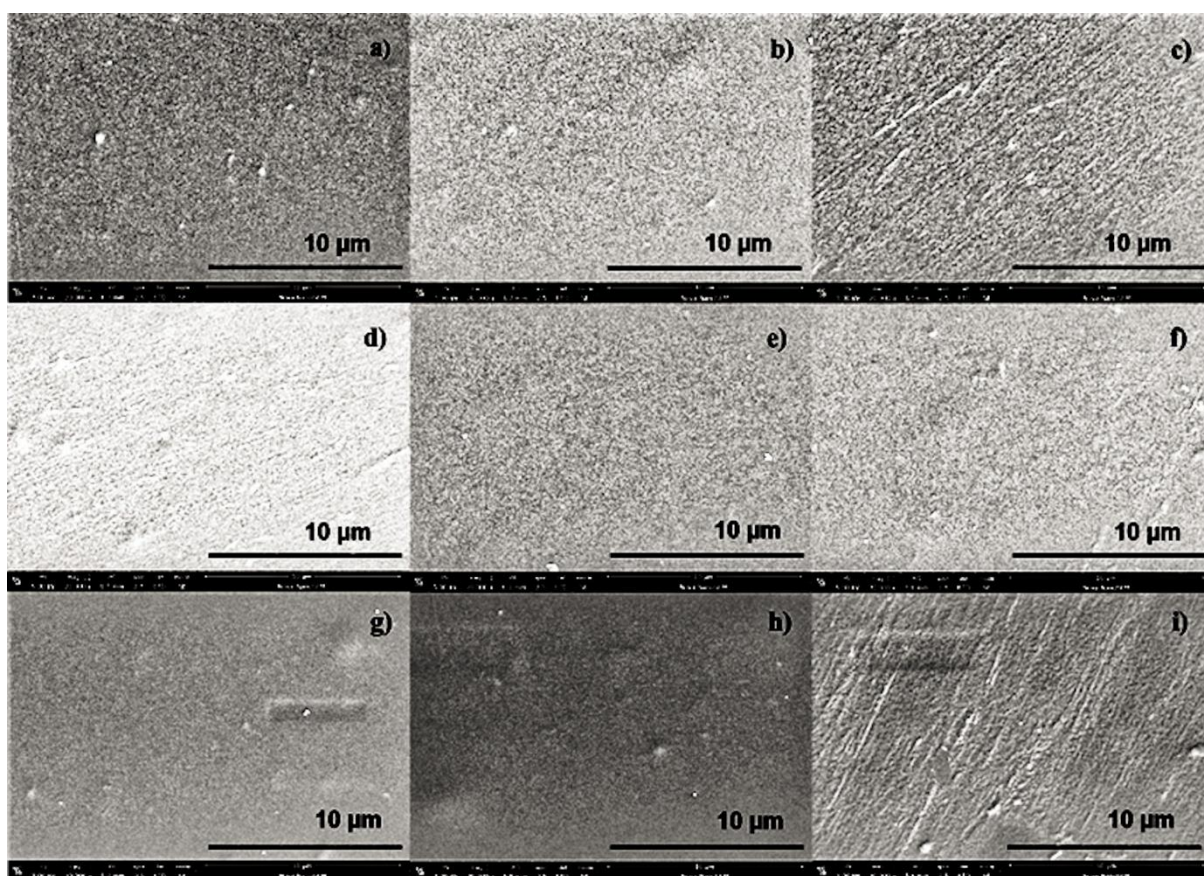


Figure 10 SEM micrographs of (a) untreated PET, (b) PET_DC, (c) DC_MAAM, (d) MAAM_1000, (e) MAAM_8500, (f) MAAM_KAPA, (g) DC_1000, (h) DC_8500 and (i) DC_KAPA

Among the surfaces treated with polysaccharides, the furcellaran-coated PET surface (Figure 10-(d,e,g,h)) exhibited a more uniformly distributed layer, facilitating consistent adhesion and growth of fibroblasts on the surface. In contrast, the PET surface coated with κ -carrageenan (Figure 10-(i)) displayed a somewhat heterogenous surface, which could potentially influence the behavior of adhering cells. Similarly, the PET surface modified with MAAM displayed an irregular and rough morphology, which is desirable for subsequent immobilization purposes⁴⁷.

Biological activity

The immobilized samples exhibited a notably weak antibacterial effect when compared to the PET reference. There is limited available research on the antimicrobial properties of carrageenans. The antimicrobial effects of three carrageenans were examined, demonstrating a significant inhibitory impact on various bacterial strains. This study also suggested that the removal of sulfate residues led to the loss of the bacteriostatic effect of ι -carrageenan, implying the essential role of sulfate residues in this effect. Additionally, the presence of carrageenan led to a concentration-dependent reduction in bacterial growth rate, albeit with a bacteriostatic rather than bactericidal effect¹⁰³. However, the inhibitory mechanism was likely not solely dependent on sulfate content but also on the underlying inhibitory mechanisms, which require further investigation. PVA- κ -carrageenan films crosslinked with glutaraldehyde exhibited no antibacterial performance unless loaded with antibacterial agents¹⁰⁴. Given these studies, the lower sulfate content of furcellaran and the unmodified nature of immobilized polysaccharides might contribute to the limited antibacterial activity observed. Additionally, the amount of immobilized furcellaran and κ -carrageenan on the PET surface might not reach the minimum inhibitory concentration (MIC).

In light of these results, it is apparent that furcellaran may not be regarded as a promising antibacterial agent on its own. More detailed results are published in **ARTICLE III**.

Anticoagulant activity tests indicated the ability of the treated surfaces to prolong clotting time. As seen in Table 3, the extrinsic coagulation pathway, assessed through prothrombin time (PT), remained unaffected by any of the tested samples.

In terms of activated partial thromboplastin time (aPPT), the clotting times for samples PET_DC_8500 and PET_DC_KAPA were slightly extended, indicating some interference with the intrinsic coagulation process.

As for thrombin time (TT), which measures the time taken for fibrinogen to convert to fibrin, PET_DC_KAPA exhibited the longest clotting time, surpassing the threshold for mild anticoagulant activity. Moreover, plasma-treated PET displayed prolonged clotting times above the threshold, attributed to its

hydrophilic surface, roughness and negative charge resulting from plasma treatment. These characteristics are associated with reduced protein adsorption and the activation of blood components⁵¹.

As expected, the anticoagulant activity was adversely affected by samples treated with MAAM¹⁰⁵. Out of all samples, a minor anticoagulant effect was detected in the instance of sample PET_DC_KAPA, which is likely associated with its sulfate content.

Table 3 Anticoagulant activity expressed by clotting times

| SAMPLE | PT (s) | aPTT (s) | TT (s) |
|---------------|---------------|-----------------|---------------|
| PET | 12.0±0.2 | 29.1±0.2 | 18.0±0.1 |
| PET_DC | 12.6±0.3 | 32.8±0.4 | 20.1±0.2 |
| PET_MAAM | 12.6±0.2 | 30.5±0.5 | 18.5±0.6 |
| MAAM_1000 | 12.1±0.2 | 28.8±0.7 | 18.4±0.1 |
| MAAM_8500 | 12.4±0.1 | 30.6±1.0 | 18.6±0.2 |
| MAAM_KAPA | 12.3±0.2 | 29.7±1.0 | 18.9±0.1 |
| DC_1000 | 13.0±0.2 | 32.5±0.8 | 18.7±0.2 |
| DC_8500 | 13.3±0.1 | 33.4±0.5 | 19.7±0.1 |
| DC_KAPA | 12.3±0.1 | 33.9±0.4 | 20.5±0.1 |

The cytotoxicity assessment (Figure 11) yielded values exceeding 80%. According to ISO 10993-5, if viability is reduced to < 70 % of the blank, it has a cytotoxic potential. In general, the cell viability of samples that underwent functionalization with MAAM and polysaccharides (FUR, κ-CA) demonstrated an increase compared to samples treated solely with plasma, signifying that all materials can be classified as non-toxic and cytocompatible. Numerous studies have suggested that cells exhibit a tendency to adhere to hydrophilic surfaces⁴⁷. Conversely, it has been reported that cells adhere and proliferate at the highest rate when cultured on a hydrophobic surface or with a contact angle of approximately 70 degrees¹⁰⁶. This could potentially explain why untreated PET exhibited the most favorable proliferation outcomes. In previous studies, plasma treated surfaces exhibit improved proliferation of fibroblast and endothelia cells¹⁰⁷.

As anticipated, the cell proliferation observed in furcellaran-coated samples aligns with previous research findings on other seaweed polysaccharides^{108,109}.

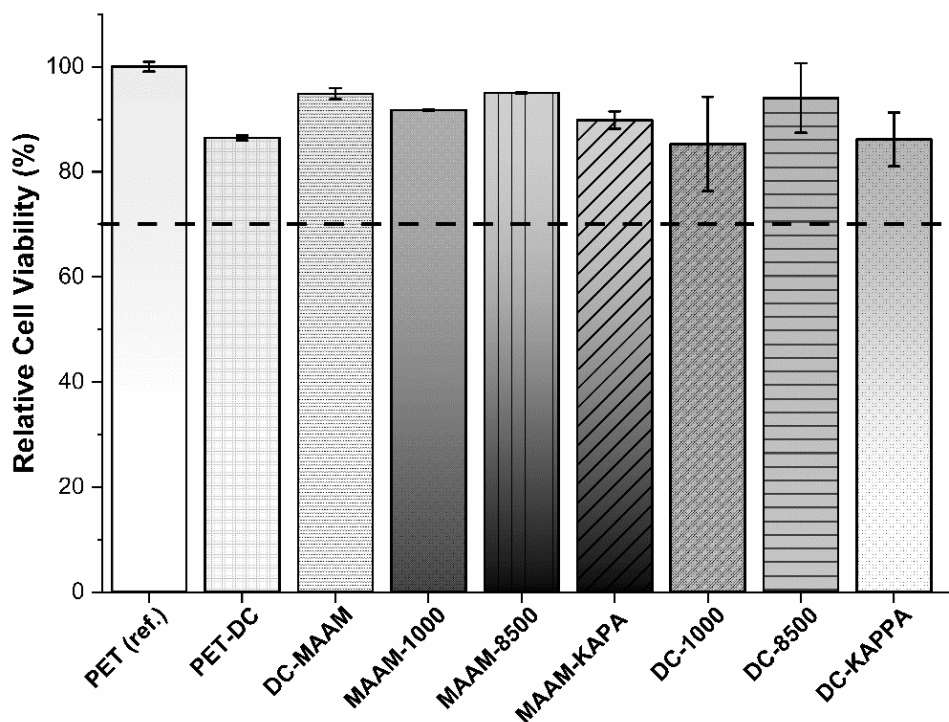


Figure 11 Relative cell viability of cells incubated with PET films coated with furcellaran of different water gel strengths (1000, 8500) and κ -carrageenan tested on a mouse embryonic fibroblast cell line (NIH/3T3).

After five days of embryonic stem cell (ESC) proliferation on uncoated (Figure 12-C) and gelatine-coated samples (Figure 12-D), no significant difference was observed between the reference (cells cultured on TPP plastic) and PET (Figure 12-A). As depicted in Figure 12-B, the cell viability on TPP plastic coated with gelatine (reference) and PET coated with gelatine did not display any significant variance. Consequently, PET was established as a suitable material for cell cultivation and was utilized as a reference in subsequent testing.

N-allylmethylamine (MAAM) treated PET films did not show any proliferation and was observed significant reduction in cell viability on sample MAAM_8500. One potential explanation for this observation is the correlation between the gel strength of FUR 8500 and insufficient interaction with the amine groups of MAAM. The gel strength of FUR 8500 was lower than that of FUR 1000, which also corresponded to the lower content of 3,6-anhydro-D-galactose residues. The amount of these units could adversely affect the immobilization of FUR 8500. Additionally, intramolecular interactions between grafted polymer brushes and polysaccharides may not have been sufficient for immobilization, negatively impacting subsequent interactions with ESCs. Another possibility is that the MAAM coating on the PET films may have interfered with the signaling pathways or biochemical cues involved in ESC proliferation.

Nevertheless, the most significant finding was that samples DC_8500 (Figure 13-B) and DC_KAPA exhibited significantly increased ESC proliferation compared to that of the reference PET (Figure 13-A). This suggests sufficient polysaccharide immobilization and its potential to enhance ESC proliferation. Notably, all gelatine-coated samples did not exhibit cytotoxic effects, except for sample MAAM_8500_G.

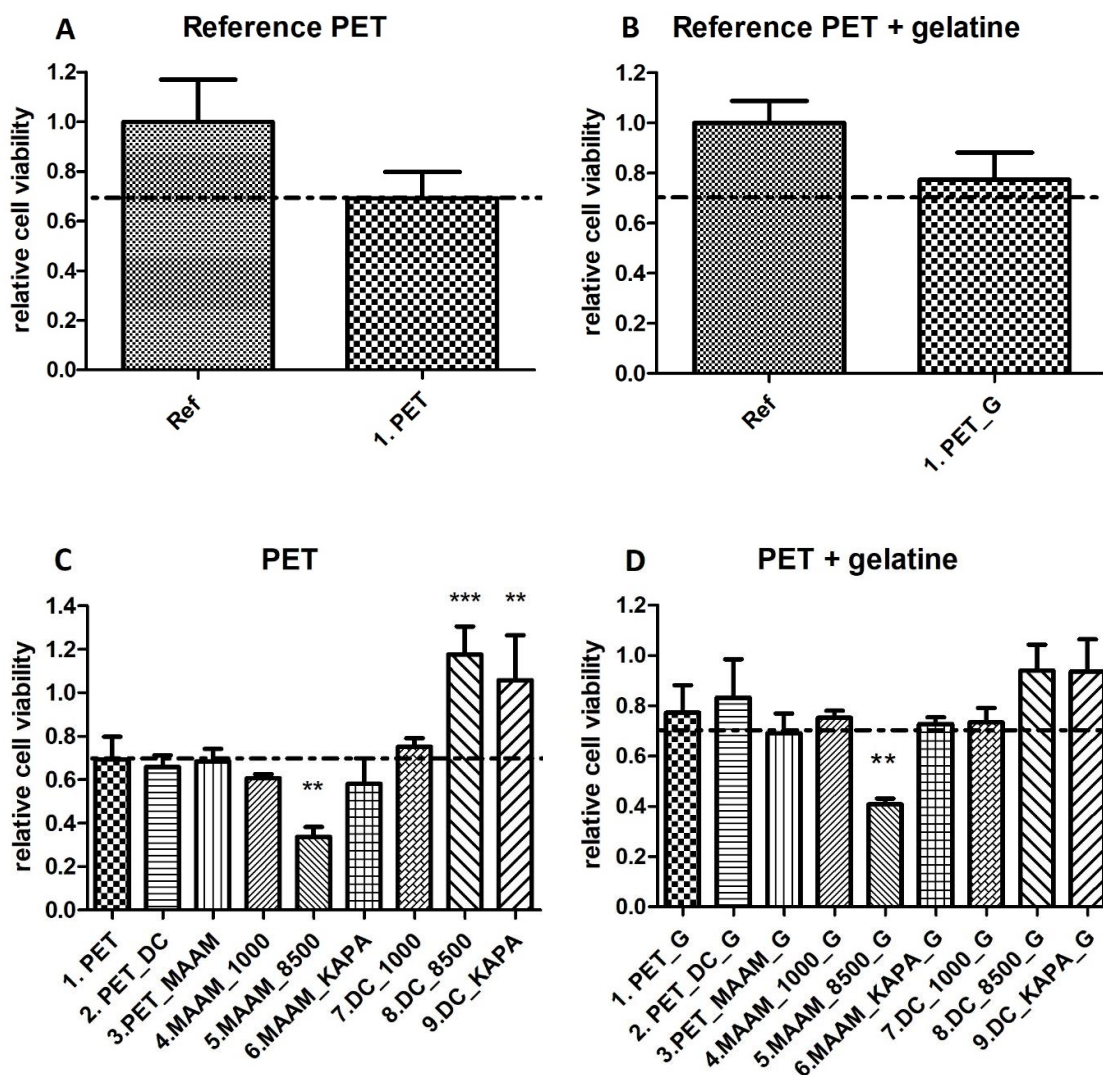


Figure 12 Cell viability in the ES R1 cell line with comparison of (A) reference (TPP) and PET; (B) TPP and PET coated with gelatine; (C) PET as a reference and samples; (D) PET and samples coated with gelatine.; * $p < 0.05$, ** $p < 0.01$, *** $p < 0.001$.

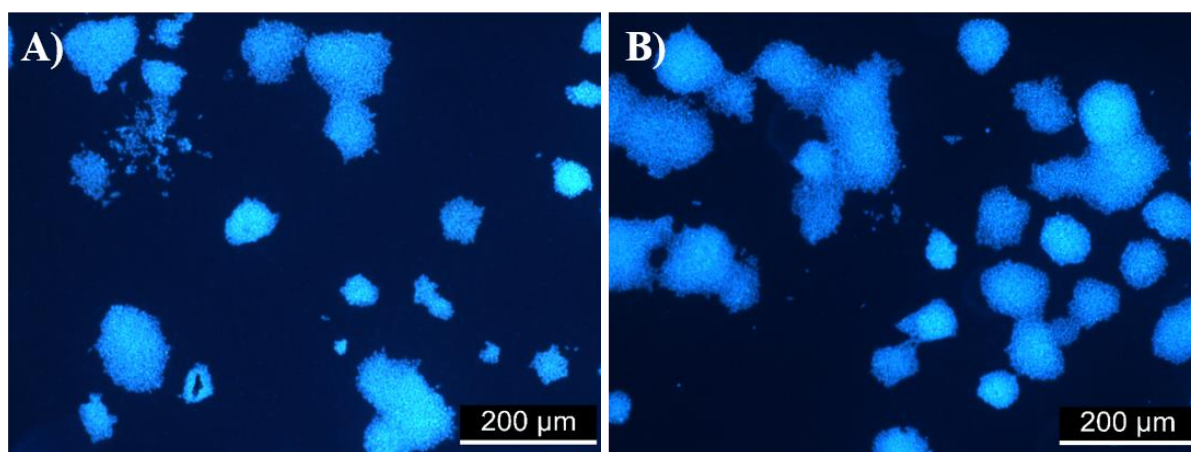


Figure 13 Mouse embryonic cells (Line R1) on A) PET uncoated with 0.1% gelatine and B) DC 8500 uncoated with 0.1% gelatine

8.1.5 Conclusion

The study conducted a comparative analysis of the immobilization of furcellaran and κ -carrageenan onto PET surfaces using a multistep approach via plasma treatment and N-allylmethylamine. The results showed that air plasma treatment significantly increased the hydrophilicity and surface energy of the PET surface, making it more suitable for subsequent immobilization. The immobilized polysaccharides exhibited an increase in hydrophobicity, but still remained less hydrophobic than the untreated PET surface. The successful immobilization of polysaccharides on the surface was supported by the presence of sulfur content.

All examined samples were found to be non-cytotoxic to the fibroblast cell line *in vitro*. Notably, samples DC_8500 and DC_KAPA exhibited significantly enhanced proliferation of embryonic stem cells compared to reference PET, suggesting potential applications of furcellaran in biomedical contexts. However, sample MAAM_8500 showed a significant reduction in cell viability, indicating the need for further investigation. The anticoagulant activity of the PET samples was also assessed, revealing that furcellaran immobilization had a slight interference with the intrinsic coagulation pathway. Conversely, no antibacterial activity was observed in any of the tested samples.

In conclusion, the findings of this study suggest that furcellaran holds promise for use in biomedical applications, thereby paving the way for the development of novel materials endowed with unique properties and potential applications in the field.

8.2 Chemical modification of furcellaran for enhanced blood compatibility

Cardiovascular illnesses are a significant public health concern, and the most common diagnoses are venous thromboembolism (VTE) and acute coronary syndrome (ACS), both of which occur from the formation of blood clots in veins or arteries. Heparin has been used as a conventional therapy for thromboembolic diseases for more than 50 years. However, its limits, as well as the 2008 contamination crisis, have prompted the search for alternate medications¹¹⁰. Sulfation has emerged as a powerful method of producing semi-synthetic heparin-like products from non-mammalian polysaccharides using the glycosaminoglycan (GAG) strategy.

Algal polysaccharides have received a lot of interest as a prospective source of natural compounds that could potentially replace the much-needed heparin product. These polysaccharides' sulfation pattern functions as a functional code that can convey a variety of biological actions⁸⁹. As a result, research has concentrated on modifying their sulfate distribution and selectively adding sulfate groups to non-sulfated polysaccharides, with the goal of increasing their therapeutic and biological relevance. Ongoing research in this area is expected to become increasingly important as sustainable processes and renewable resources gain more emphasis.

Furcellaran, a naturally sulfated polysaccharide derived from marine algae, is a feasible substrate for the enhancement of unique properties, notably against thrombus formation. To introduce sulfate groups into furcellaran with the goal of achieving the desired degree and pattern of sulfation, several methods can be used, including chlorosulfation, sulfur trioxide with pyridine, and sulfuric acid methods, and sulfamic acid in the presence of dissolved activators or deep eutectic solvent, with activators such as DCC or DMAP^{79,111}.

In this study, chlorosulfonic acid, $\text{SO}_3\cdot\text{Py}$ complex and sulfuric acid with DCC were chosen based on their well-established track record in the literature, availability, hence for consistency and comparability with previous studies. The biological activity of the polysaccharide will be then reflected by various structural parameters such as the degree of sulfation (DS), molecular weight, sulfation position, sugar type, and glycosidic bond.

The aim is to compare the effectiveness of the used methods and subsequently test the hemocompatibility of the sulfated product. Results will serve as a jumping off point to implement novel methods for further optimization and to acquire well-defined sulfated products with desired properties.

8.2.1 Preparation

Sulfation of furcellaran

The sulfation of furcellaran was preceded by obtention of FUR in a pyridinium salt form using Amberlite IR 120⁺ cation exchange column. The eluate was neutralized by pyridine (pH 7-8), dialyzed and lyophilized. Sulfation (Figure 14) by SO₃·Py complex was proceeded as follows: FUR was dissolved in anhydrous DMSO/DMF by stirring at room temperature for 30 min, and then SO₃·Py complex in molar ratio 4:1 to sugar unit was added. The mixture was heated at 70 °C for 3 hours, then poured into ice water and neutralized with 1 M NaOH. Afterwards, it was precipitated, dialyzed, and lyophilized to yield FUR_DMSO or FUR_DMF. To employ chlorosulfonic acid method, FUR was added to a three-necked flask containing anhydrous DMF (30 mL) and 2 mL of chlorosulfonic acid added dropwise with cooling. The reaction mixture was heated at 60°C for 2 h. The resulting solution was neutralized, precipitated and dialyzed. The final product, sample FUR_HSO3CL, was obtained after freeze-drying. Sulfation via H₂SO₄ and DCC was performed in the following manner: FUR was dissolved in anhydrous DMF with DCC (4:1 to sugar unit) dissolved in DMF. 96% H₂SO₄ was added dropwise and the reaction mixture was kept at 0 °C for 30 min. The mixture was neutralized, filtered, and dialyzed. The sample FUR_DCC, was obtained after lyophilization.

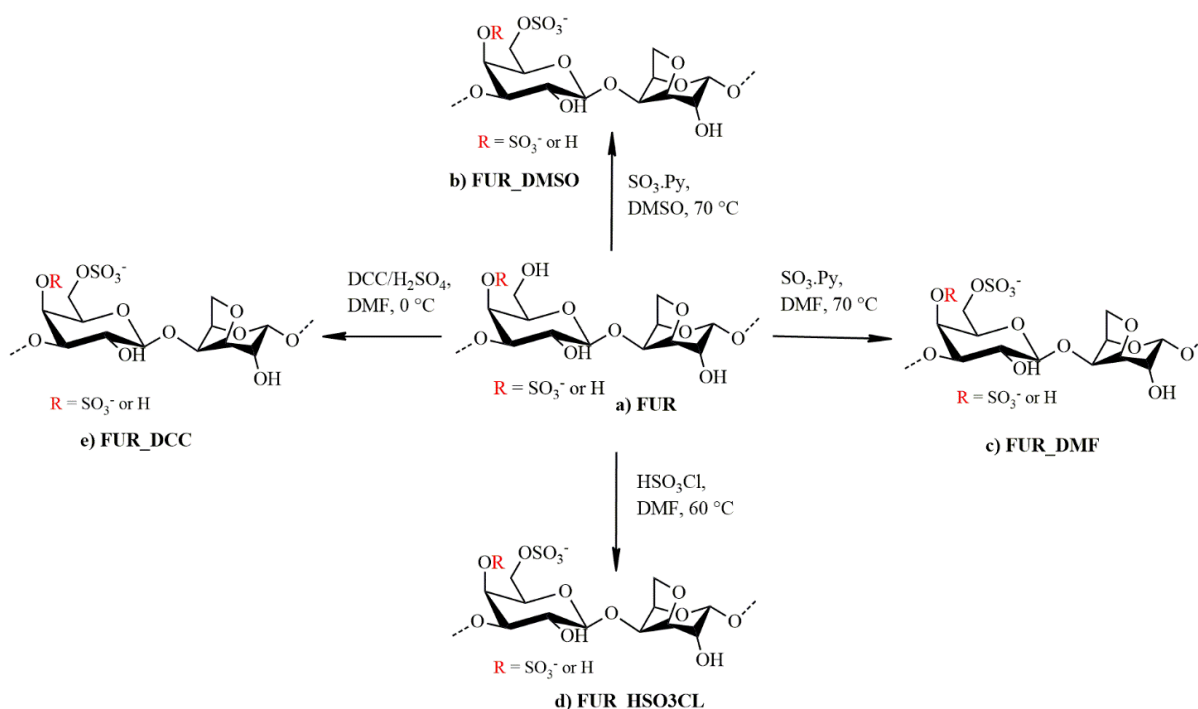


Figure 14 Schematic representation of sulfation methods with targeted sulfate position. The structures do not reflect the strict composition of the sample

8.2.2 Characterization of sulfated derivatives

The native and sulfated furcellaran samples were characterized using FTIR, Gel Permeation Chromatography (GPC), elemental analysis (Flash 2000 CHNS/O), and XPS. For a comprehensive understanding of the methodology employed, details are provided in the relevant article (**ARTICLE IV**).

8.2.3 Evaluation of hemocompatibility

The anticoagulant activity was carried out in collaboration with KNTB Hospital, and cytotoxicity testing was assessed in cooperation with Prof. Humpolíček's research group at CPS, following ISO standard 10993 for the biological evaluation of medical devices. The platelet adhesion test was conducted in partnership with Pavol Jozef Šafárik University in Košice. For detailed information on the biological evaluation of the prepared samples, see (**ARTICLE IV**)

8.2.4 Results and Discussion

The utilization of FT-IR spectroscopy facilitated the characterization of native furcellaran and its sulfated derivatives. The spectra obtained from this examination, as depicted in Figure 15, revealed a multitude of absorption peaks.

As depicted in Figure 15-A. The O-H stretching signal was observed at approximately 3400 cm^{-1} , and the asymmetric C-H stretch band of the saccharide ring was noted at 2920 cm^{-1} . Additionally, a band at 1650 cm^{-1} was attributed to water deformation.

For native furcellaran, a single band appeared at 845 cm^{-1} (Figure 15-B,D), corresponding to the axial galactose-4-sulfate. Following sulfation, a new absorption band emerged at 820 cm^{-1} (Figure 15-B,D), which can be assigned to C-O-S of galactose-6-sulfate¹¹², and the peak associated with galactose-4-sulfate became less prominent. This phenomenon may be attributed to the susceptibility of the polysaccharide to the sulfation methods employed. In the case of FUR_DCC (Figure 15-D), sulfated groups were distributed proportionally between the G4 and G6 positions. However, the intensity of these bands was relatively low compared to other samples.

In general, chemical sulfation can lead to partial cleavage, resulting in a reduction in the molecular weight (M_w) of the resulting polymer as shown in Table 4. As seen, high PDI of the furcellaran pyridinium salt was observed due to various factors, such isolation and purification as well as the inherent polydispersity of native furcellaran itself. The decrease of M_w could be attributed to the removal of impurities through precipitation, dialysis and an acidic character of sulfating agents. M_w of oversulfated derivatives ranged from 12,473 to 2,720 Da,

representing a noticeable decline compared to unmodified furcellaran. The use of sulfating agents such as HSO_3Cl or H_2SO_4 during sulfation likely led to the degradation of the polysaccharide more likely in a radical mechanism. These highly reactive and hygroscopic reagents in an acidic environment could result in unwanted hydrolysis and partial degradation of the furcellaran backbone¹¹³. Besides the molar ratio of reagent to sugar unit used, the major factor contributing to the degradation is temperature and reaction time. More detailed results are published in **ARTICLE IV**.

Since the 3,6-anhydro- α -galactosidic bond in furcellaran's structure is susceptible to acidic conditions, its presence is closely associated with depolymerization¹¹⁴. The existence of the 3,6-anhydro-galactosidic bond was confirmed by a band at 930 cm^{-1} (Figure 15-B) in all sulfated samples, although the band's intensity was lower compared to native furcellaran. Notably, the sample FUR_HSO3CL exhibited the least intense band, indicating a partial disruption of the galactosidic bond. Another band at 1060 cm^{-1} (Figure 15-B, C) was attributed to C-O stretching vibrations of sulfate ester groups. The most intense band, observed at 1220 cm^{-1} (Figure 15-B,C), indicated the total sulfate content¹¹⁵.

The elemental analysis data presented in Table 4 confirmed that oversulfated furcellaran samples exhibited a significant increase in sulfur content compared to parental polysaccharide, where FUR_HSO3CL has the highest DS.

Table 4 Molecular weight and elemental composition and degree of sulfation of tested samples

| Sample | M_w (Da) | Elements (%w/w) | | | | | DS ^a |
|------------|------------|-----------------|---------------|---------------|-----|------|-----------------|
| | | C | S | H | N | | |
| FUR | 131 534 | 31.5 ± 0.4 | 2.0 ± 0.2 | 4.9 ± 0.3 | 0.1 | 0.15 | |
| FUR_DMSO | 12 473 | 22.8 ± 0.1 | 8.0 ± 0.1 | 4.1 ± 0.2 | 1 | 0.8 | |
| FUR_DMF | 7 648 | 21.7 ± 0.1 | 8.2 ± 0.3 | 4.2 ± 0.2 | 0.8 | 0.53 | |
| FUR_HSO3CL | 2 720 | 16.8 | 6.9 ± 0.3 | 2.8 | 0.4 | 0.91 | |
| FUR_DCC | 4 816 | 25.7 ± 0.2 | 3.2 ± 0.2 | 4.2 | 0.8 | 0.28 | |

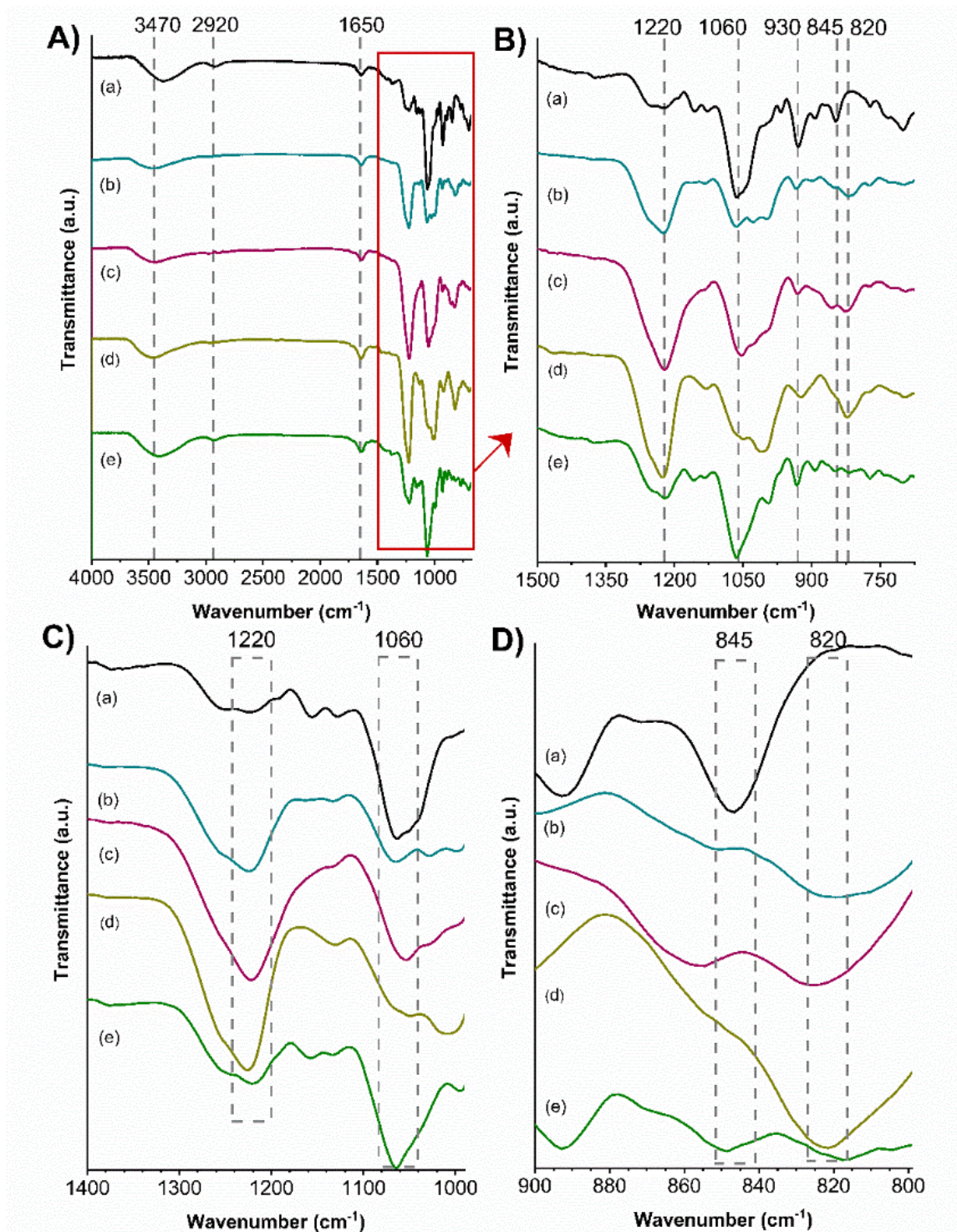


Figure 15 Attenuated total reflectance (ATR)-FT-IR spectrum collected from the samples. Spectrum (a) is for FUR, spectrum (b) is for FUR_DMSO, spectrum (c) is for FUR_DMF, spectrum (d) is for FUR_HSO3CL and spectrum (e) is for FUR_DCC.

The figure 16 a) illustrates a comparison of the complete carbon peaks for all examined samples. The inset provides a detailed deconvolution of the C 1s peak for the FUR sample, which is further divided into five components, located at approximately 284.6, 285.0, 286.3, 287.8, and 289.0 eV, respectively. The component at around 284.6 eV corresponds to hydrocarbon C-C/C-H bonds, while the component at 285.0 eV relates to C-S chemical bonds. As depicted in Figure 16 b), all samples display spin-orbit sulfur splitting S2p1/2 and S2p3/2 at pñ 169.1 eV and 167.7 eV, respectively. These binding energies are characteristic of the sulfate group and remain consistent across various reaction conditions.

The components centered at a binding energy of approximately 286.3 eV, 287.8 eV, and 289.0 eV are associated with oxygen-containing functional groups, specifically C-O, C=O, and O-C=O, respectively. The presence of the C=O group may suggest potential oxidation of the polysaccharide, which might be attributed to alkali treatment during the extraction or storage and reaction conditions. More detailed results are published in **ARTICLE IV**.

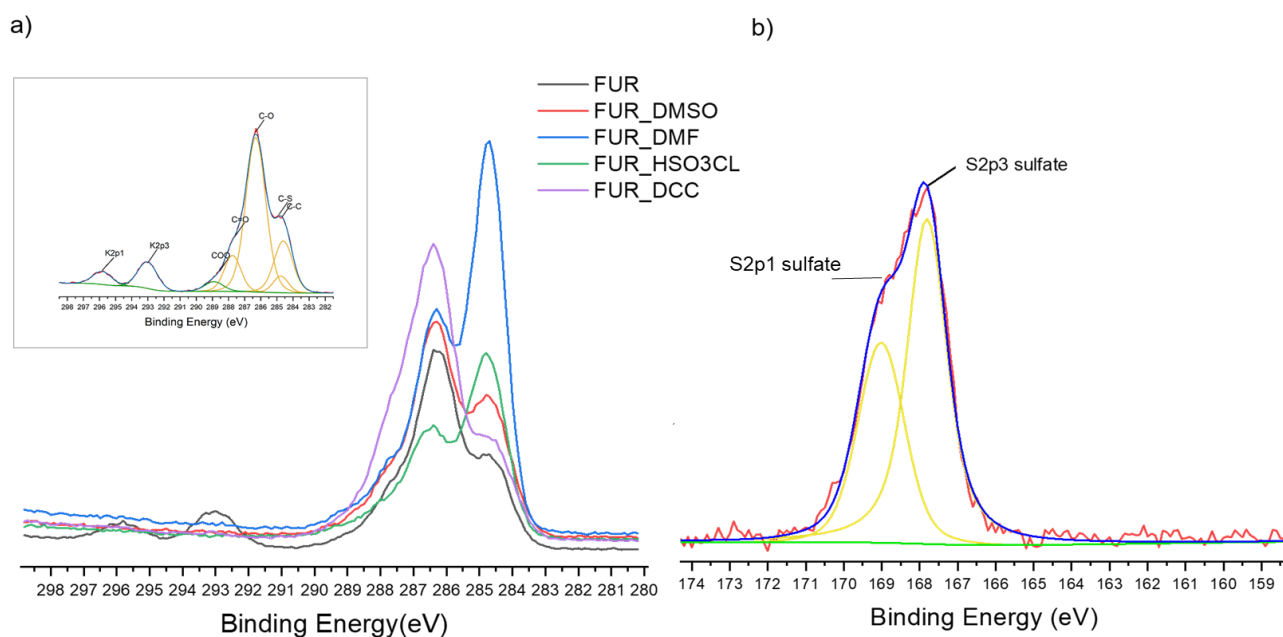


Figure 16 XPS spectra: a) overlay of the high-resolution C 1s scans for furcellaran and its derivatives. Inset displays the results of C 1s deconvolution for FUR sample, b) binding of sulfate for FUR_DMSO as a representative sample

The cytotoxicity of native furcellaran and its oversulfated derivatives (Figure 17) was tested in the concentration range of 0.1-2 mg/mL. All samples reduced cell

viability in a dose-dependent manner, but none were cytotoxic at concentrations up to 0.1 mg/mL. Native furcellaran was less cytotoxic than sulfated derivatives, with viability reaching 76.8% at 1 mg/mL. Higher DS values were found to be more likely to contribute to cytotoxicity, but among the oversulfated samples, no direct relationship between DS and cytotoxic activity was observed. For SO₃·Py complex reaction, two different solvents, DMSO and DMF were utilized to leverage their distinct nucleophilic properties to achieve varying degree of sulfation. Despite to presumed stronger nucleophilic ability and lower cell growth inhibition of DMSO solvent^{116,117}, both FUR_DMSO and FUR_DMF samples demonstrated comparable cell viability outcomes. The introduction of sulfate groups on the G-6 position caused stronger cytotoxicity than on the G-4 position. This is in accordance with Liang et al., demonstrating a 2-fold decrease in HUVEC cell viability after treatment with the oversulfated κ-carrageenan (1 mg/mL) compared to unmodified κ-carrageenan¹¹⁸. Higher cytotoxicity in oversulfated samples may be due to a combination of high DS, lower *M_w*, and sulfation position compared to unmodified furcellaran, as the negatively charged membrane surface prevented interactions between furcellaran and cells.

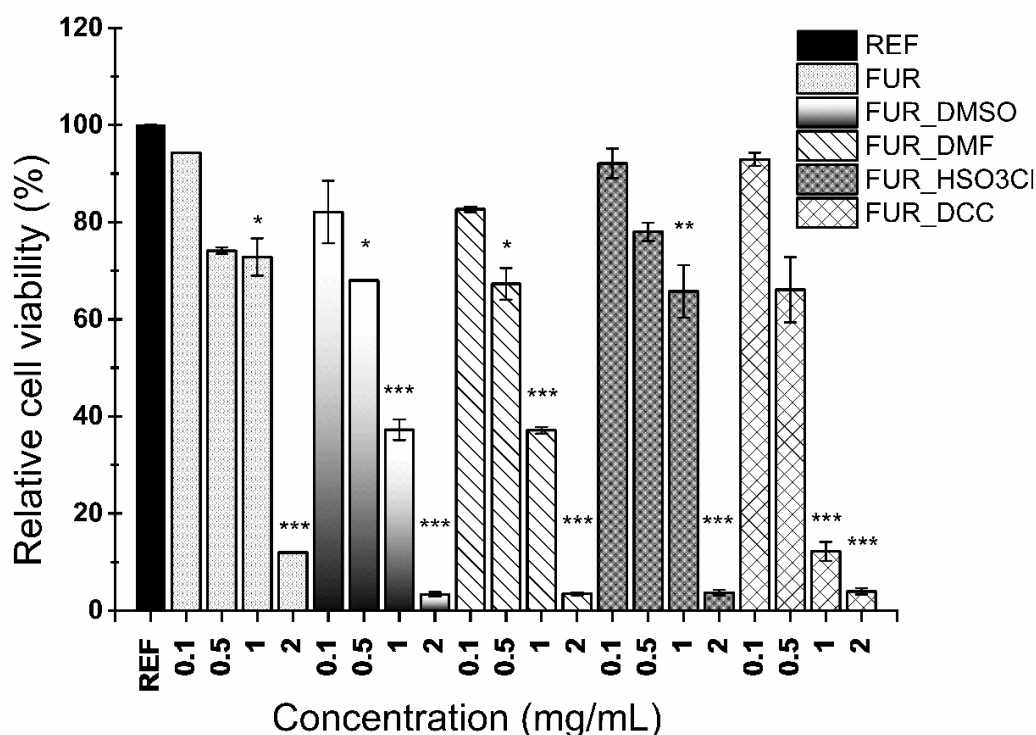


Figure 17 Relative cell viability values expressed as a percent of control (expanded polystyrene); * $p < 0.05$, ** $p < 0.01$, *** $p < 0.001$

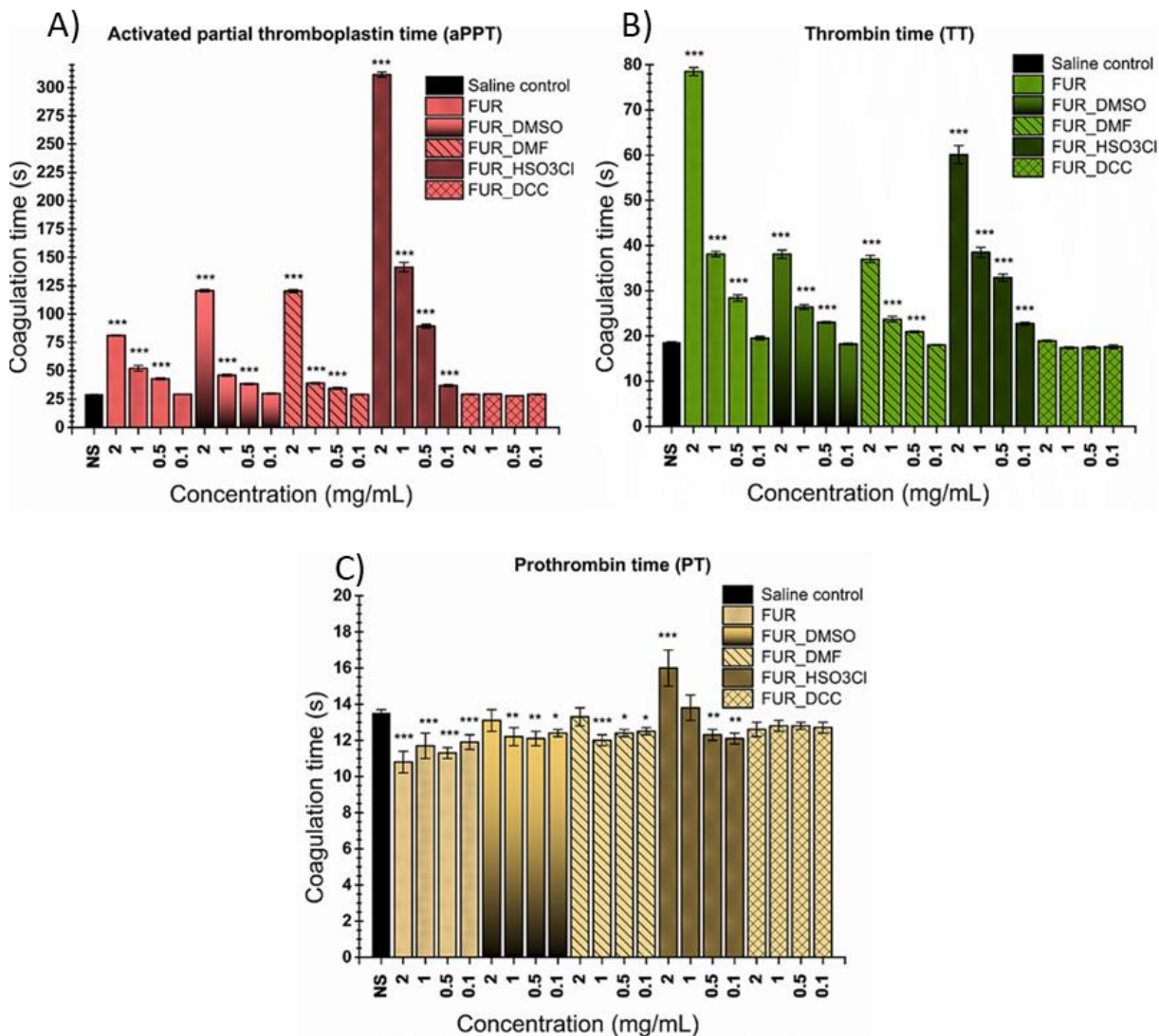


Figure 18 Anticoagulation activity results; A) aPTT: activated partial thromboplastin time; B) TT: thrombin time; C) PT: prothrombin time. The significant differences compared to the control group (NS: negative control, saline solution) are designated as * $p < 0.05$; ** $p < 0.01$; *** $p < 0.001$. The clotting time of saline solution in the PT, APTT and TT assays was 13.5 s, 29.1 s, and 18.5 s, respectively. No coagulation response was observed for sodium heparin (positive control) across the range of concentrations tested.

Native furcellaran and its sulfated derivatives demonstrated a dose-dependent prolongation of clotting time (Figure 18) in the aPPT and TT assays, except for FUR_DCC. Despite a higher sulfur content in comparison to native furcellaran, subtle variations in the arrangement and distribution of sulfated residues along the galactan backbone might be accountable for the interaction among proteases, inhibitors, and coagulation system activators, leading to procoagulant effects¹¹⁹.

Therefore, variances in the degree and pattern of sulfation along the polysaccharide chain could explain the results observed for FUR_DCC.

FUR_HSO3CL exhibited the highest anticoagulant activity, with a 4-fold increase compared to native furcellaran in aPPT assay. Saluri et al.¹²⁰ revealed λ -carrageenan has an enhanced anticoagulant effect when the molecular weight is significantly reduced compared to the native sample. This implies that carrageenans may demonstrate their optimal efficacy within a specific molecular weight range. The significant prolongation of aPPT time observed for native FUR highlights that its comparatively elevated molecular weight might increase the likelihood of effective collisions. This is due to the longer chain possessing a greater number of repeating units and higher valence, enabling it to bind to a larger number of receptors¹²¹. The sulfate content was identified as the major factor responsible for prolonging the intrinsic pathway, however effect of polysaccharides on fibrin formation depends on the overall structural features of polysaccharide, as interaction with coagulation cofactors and their target proteases and inhibitors were determined to be very stereospecific¹²². According to Liang and Maio¹²³, a sulfate ester at the G4 position seemed to be more efficient.

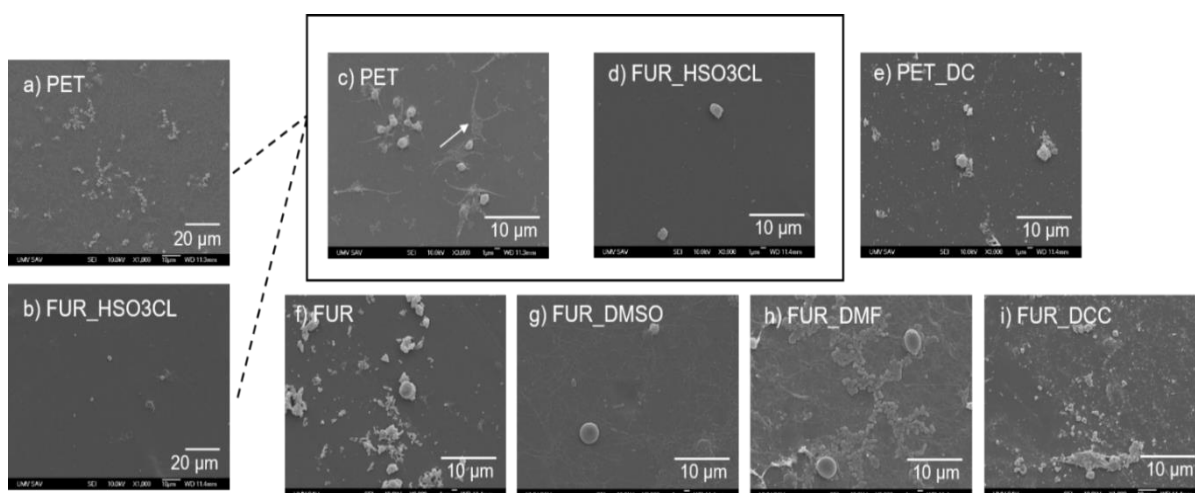


Figure 19 Morphology of platelets a) untreated PET, b) FUR_HSO3CL c) untreated PET, d) FUR_HSO3CL, e) Air plasma treated PET_DC, f) FUR, g) FUR_DMSO, h) FUR_DMF, i) FUR_DCC. Two different magnifications are shown: $1000\times$ (a, b) and $3000\times$ (c–i).

Tested samples were found to act only on the intrinsic pathways of the blood coagulation system, which is reflected in their insignificant prolongation of clotting time in the prothrombin time (PT) assay. Among the all tested samples, FUR_HSO3CL showed itself to be potent anticoagulant agent in PT assay, likely as a result of considerably reduce M_w (2.7 kDa) during the sulfation along with high DS. In study of Melo et al.¹²⁴, the low molecular weight fractions from the

sulfated galactan of *Botryocladia occidentalis* showed high anticoagulant activity, and the total thrombin inhibition mediated by the heparin cofactor II was even stronger than that of the parent polysaccharide. Thus, the coagulation inhibition profile resembling that of heparin, by facilitating the neutralization of factor Xa and thrombin through the endogenous coagulation inhibitor antithrombin¹²⁵. Elevated DS enhances the density of negative charges, thereby inhibiting the activity of IIa and Xa. The results of aPPT and TT assays also indicate that anticoagulant behavior is influenced not only by the high sulfate density but also by factors such as molecular size, the position of sulfate groups, and other structural characteristics.

The presence and morphology of platelets adhered to the samples were estimated by SEM (Figure 19) that reveal a noticeable difference between the untreated PET sample and the treated ones.

As anticipated, the untreated PET surface (Figure 19 – a, c)) exhibits activated blood platelets characterized by dendritic spreading, hyalomere, and an intermediate pseudopodia network. After RF air plasma discharge activation (FUR_DC), only a few platelets in a non-activated, round shape were detected on the surface (Fig. 19e)). Such a phenomenon can be explained by the introduced oxygen functional groups and higher hydrophilicity of the surface, which is less favorable for the adsorption of proteins. A predominance of inactivated platelets of spherical shape without platelet aggregation was found on the surface treated with native furcellaran (Fig. 19f)). However, some undetectable particles were entrapped in the vicinity of platelets which may originate from the PRP itself. Platelet aggregates were observed in the case of FUR_DCC (Fig. 19i)), which are well-known to be critical for hemostatic plug formation and thrombosis. Conversely, surfaces subjected to highly sulfated furcellaran derivatives (Fig. 19b), d, g-i)) exhibited a notable reduction in platelet adhesion, along with the absence of the most activated platelet stages on the pathway to full spreading. Only some resting platelets with discoid shape and few inactivated spherical platelets were observed indicating the excellent anti-platelets adhesion property and potential antithrombotic characteristics.

8.2.5 Conclusion

In the second part of the research, four different methods of sulfation were used to enhance the hemocompatibility of furcellaran, resulting in derivatives with varying degrees of sulfation and low molecular weight. The sulfated furcellaran derivatives showed a dose-dependent increase in cytotoxicity, which was attributed to the sulfation process. The furcellaran sulfate produced using chlorosulfonic acid had the highest sulfate content and had a significant impact on the anticoagulant activity, which was directly proportional to the sulfate

content and low molecular weight. The furcellaran sulfates produced using $\text{SO}_3\cdot\text{Py}$ complex showed significant effects on both the intrinsic and common pathways of the coagulation cascade, regardless of the solvent used. The native furcellaran was most effective in retarding fibrin formation, suggesting that the stereochemistry of the polysaccharide may also play a role in the final step of the clotting cascade, in addition to the sulfate content. All oversulfated samples exhibited an excellent anti-platelet activity. However, the furcellaran derivative produced using dicyclohexylcarbodiimide did not show any beneficial effects on coagulation and antiplatelets adhesion likely due to its low sulfate content and molecular weight. The study indicates that sulfation has the potential to improve the hemocompatibility of furcellaran and may be a promising candidate for anticoagulant therapy after further optimization.

SUMMARY OF WORK AND CONTRIBUTION TO SCIENCE

The progression of the field of biomaterials science stands as a critical pursuit, especially when addressing intricate challenges associated with interfacial biocompatibility, antibacterial properties, and hemocompatibility within the realm of biomedical applications. The use of polysaccharide polymers derived from diverse algal species has emerged as a promising avenue to tackle these intricate issues.

Sulfated seaweed polysaccharides have garnered significant attention due to their several biological activities, with their sulfate pattern acting as a code able to transmit functional information. Among these polysaccharides, furcellaran, derived from the red algae *Furcellaria lumbricalis*, stands out as a compelling candidate. While furcellaran has traditionally been the subject of research primarily focused on its prospective applications in packaging materials and its role in the food industry, it is of paramount importance to emphasize the limited extent of prior investigations aimed at uncovering its prospective role in the broader biomedical context.

One significant scientific contribution lies in the study of immobilizing furcellaran onto PET surfaces through multistep approach. This intricate methodology involves grafting N-allylmethylamine onto a functionalized PET surface through air plasma treatment, followed by anchoring furcellaran as a bioactive agent. Through analysis of surface characteristics employing contact angle measurements, XPS, SEM, a comprehensive understanding of the resulting modified surfaces was achieved.

The impact of these surface modifications on biomedical applications was investigated through a series of rigorous cell interaction assays. These included assessments of antibacterial activity, anticoagulant activity, and cytocompatibility with fibroblasts and stem cells, Notably, furcellaran-coated PET films exhibited a remarkable enhancement in embryonic stem cell (ESC) proliferation *in vitro*, underscoring their promise in promoting cell growth.

Furthermore, a parallel line of research focused on the sulfation of furcellaran, an endeavor that holds significant implications for its anticoagulant properties. Various sulfation methods were explored, each yielding furcellaran derivatives with different DS and M_w . *In vitro* clotting assays illuminated the role of sulfate esters in conferring anticoagulant activity. The results demonstrated the potential of sulfated furcellaran derivatives to interfere with intrinsic coagulation pathway, offering substantial anticoagulant efficacy. Importantly, these sulfated derivatives showed non-cytotoxic behavior up to a concentration of 0.1 mg/mL and exhibited a substantial reduction in platelet adhesion, further substantiating their

hemocompatibility. These findings afford the opportunity to infer the effectiveness of applied methodologies, as well as contemplate their prospective optimization.

In summary, these research efforts collectively advance our understanding of the role of furcellaran and its sulfated derivatives in biomedical applications. The systematic surface modifications and comprehensive characterizations pave the way for enhanced interfacial biocompatibility and hemocompatibility, as well as the potential for novel therapies. These findings contribute significantly to the evolving field of biomaterials science, offering promising avenues for addressing critical challenges in healthcare and medical device development.

REFERENCES

- (1) D' Ayala, G. G.; Malinconico, M.; Laurienzo, P. Marine Derived Polysaccharides for Biomedical Applications: Chemical Modification Approaches. *Molecules* **2008**, *13* (9), 2069–2106. <https://doi.org/10.3390/molecules13092069>.
- (2) Lee, K. Y.; Mooney, D. J. Alginate: Properties and Biomedical Applications. *Progress in Polymer Science* **2012**, *37* (1), 106–126. <https://doi.org/10.1016/j.progpolymsci.2011.06.003>.
- (3) Wijesinghe, W. A. J. P.; Jeon, Y.-J. Biological Activities and Potential Industrial Applications of Fucose Rich Sulfated Polysaccharides and Fucoidans Isolated from Brown Seaweeds: A Review. *Carbohydrate Polymers* **2012**, *88* (1), 13–20. <https://doi.org/10.1016/j.carbpol.2011.12.029>.
- (4) Beaumont, M.; Tran, R.; Vera, G.; Niedrist, D.; Rousset, A.; Pierre, R.; Shastri, V. P.; Forget, A. Hydrogel-Forming Algae Polysaccharides: From Seaweed to Biomedical Applications. *Biomacromolecules* **2021**, *22* (3), 1027–1052. <https://doi.org/10.1021/acs.biomac.0c01406>.
- (5) Ozaltin, K.; Lehocky, M.; Humpolicek, P.; Pelkova, J.; Di Martino, A.; Karakurt, I.; Saha, P. Anticoagulant Polyethylene Terephthalate Surface by Plasma-Mediated Fucoidan Immobilization. *Polymers* **2019**, *11* (5), 750. <https://doi.org/10.3390/polym11050750>.
- (6) Pires, A. L. R.; Bierhalz, A. C. K.; Moraes, Â. M. BIOMATERIALS: TYPES, APPLICATIONS, AND MARKET. *Quím. Nova* **2015**, *38*, 957–971. <https://doi.org/10.5935/0100-4042.20150094>.
- (7) Rahmati, M.; Pennisi, C. P.; Budd, E.; Mobasheri, A.; Mozafari, M. Biomaterials for Regenerative Medicine: Historical Perspectives and Current Trends. *Adv Exp Med Biol* **2018**, *1119*, 1–19. https://doi.org/10.1007/5584_2018_278.
- (8) Todros, S.; Todesco, M.; Bagnò, A. Biomaterials and Their Biomedical Applications: From Replacement to Regeneration. *Processes* **2021**, *9* (11), 1949. <https://doi.org/10.3390/pr9111949>.
- (9) Kasiński, A.; Zielińska-Pisklak, M.; Oledzka, E.; Sobczak, M. Smart Hydrogels - Synthetic Stimuli-Responsive Antitumor Drug Release Systems. *Int J Nanomedicine* **2020**, *15*, 4541–4572. <https://doi.org/10.2147/IJN.S248987>.
- (10) Biswal, T.; BadJena, S. K.; Pradhan, D. Sustainable Biomaterials and Their Applications: A Short Review. *Materials Today: Proceedings* **2020**, *30*, 274–282. <https://doi.org/10.1016/j.matpr.2020.01.437>.
- (11) Subramaniam, A.; Sethuraman, S. Chapter 18 - Biomedical Applications of Nondegradable Polymers. In *Natural and Synthetic Biomedical Polymers*; Kumbar, S. G., Laurencin, C. T., Deng, M., Eds.; Elsevier: Oxford, 2014; pp 301–308. <https://doi.org/10.1016/B978-0-12-396983-5.00019-3>.
- (12) Lyu, S.; Untereker, D. Degradability of Polymers for Implantable Biomedical Devices. *Int J Mol Sci* **2009**, *10* (9), 4033–4065. <https://doi.org/10.3390/ijms10094033>.
- (13) Gunatillake, P. A.; Adhikari, R. 2 - Nondegradable Synthetic Polymers for Medical Devices and Implants. In *Biosynthetic Polymers for Medical Applications*; Poole-Warren, L., Martens, P., Green, R., Eds.; Woodhead Publishing Series in Biomaterials; Woodhead Publishing, 2016; pp 33–62. <https://doi.org/10.1016/B978-1-78242-105-4.00002-X>.

- (14) Kim, S.; Liu, S. Smart and Biostable Polyurethanes for Long-Term Implants. *ACS Biomater. Sci. Eng.* **2018**, *4* (5), 1479–1490. <https://doi.org/10.1021/acsbiomaterials.8b00301>.
- (15) Daghighi, S.; Sjollem, J.; van der Mei, H. C.; Busscher, H. J.; Rochford, E. T. J. Infection Resistance of Degradable versus Non-Degradable Biomaterials: An Assessment of the Potential Mechanisms. *Biomaterials* **2013**, *34* (33), 8013–8017. <https://doi.org/10.1016/j.biomaterials.2013.07.044>.
- (16) Xiao Peng; Kai Dong; Zhiyi Wu; Jie Wang; Zhong Lin Wang. A Review on Emerging Biodegradable Polymers for Environmentally Benign Transient Electronic Skins. *Journal of materials science* **2021**, *56* (30), 16765–16789. <https://doi.org/10.1007/s10853-021-06323-0>.
- (17) Balaji, A. B.; Pakalapati, H.; Khalid, M.; Walvekar, R.; Siddiqui, H. 1 - Natural and Synthetic Biocompatible and Biodegradable Polymers. In *Biodegradable and Biocompatible Polymer Composites*; Shimpi, N. G., Ed.; Woodhead Publishing Series in Composites Science and Engineering; Woodhead Publishing, 2018; pp 3–32. <https://doi.org/10.1016/B978-0-08-100970-3.00001-8>.
- (18) Zhang, Z.; Ortiz, O.; Goyal, R.; Kohn, J. 13 - Biodegradable Polymers. In *Handbook of Polymer Applications in Medicine and Medical Devices*; Modjarrad, K., Ebnesajjad, S., Eds.; Plastics Design Library; William Andrew Publishing: Oxford, 2014; pp 303–335. <https://doi.org/10.1016/B978-0-323-22805-3.00013-X>.
- (19) Joyce, K.; Fabra, G. T.; Bozkurt, Y.; Pandit, A. Bioactive Potential of Natural Biomaterials: Identification, Retention and Assessment of Biological Properties. *Sig Transduct Target Ther* **2021**, *6* (1), 1–28. <https://doi.org/10.1038/s41392-021-00512-8>.
- (20) Afshari, H.; Maleki, M.; Hakimian, M.; Tanha, R. A.; Salouti, M. Immunogenicity Evaluating of the SLNs-Alginate Conjugate against *Pseudomonas Aeruginosa*. *Journal of Immunological Methods* **2021**, *488*, 112938. <https://doi.org/10.1016/j.jim.2020.112938>.
- (21) Samir, A.; Ashour, F. H.; Hakim, A. A. A.; Bassyouni, M. Recent Advances in Biodegradable Polymers for Sustainable Applications. *npj Mater Degrad* **2022**, *6* (1), 1–28. <https://doi.org/10.1038/s41529-022-00277-7>.
- (22) Nair, L. S.; Laurencin, C. T. Biodegradable Polymers as Biomaterials. *Progress in Polymer Science* **2007**, *32* (8), 762–798. <https://doi.org/10.1016/j.progpolymsci.2007.05.017>.
- (23) Panchal, S. S.; Vasava, D. V. Biodegradable Polymeric Materials: Synthetic Approach. *ACS Omega* **2020**, *5* (9), 4370–4379. <https://doi.org/10.1021/acsomega.9b04422>.
- (24) Amini, A. R.; Wallace, J. S.; Nukavarapu, S. P. Short-Term and Long-Term Effects of Orthopedic Biodegradable Implants. *J Long Term Eff Med Implants* **2011**, *21* (2), 93–122.
- (25) Metwally, S.; Stachewicz, U. Surface Potential and Charges Impact on Cell Responses on Biomaterials Interfaces for Medical Applications. *Materials Science and Engineering: C* **2019**, *104*, 109883. <https://doi.org/10.1016/j.msec.2019.109883>.
- (26) Bose, S.; Robertson, S. F.; Bandyopadhyay, A. Surface Modification of Biomaterials and Biomedical Devices Using Additive Manufacturing. *Acta Biomater* **2018**, *66*, 6–22. <https://doi.org/10.1016/j.actbio.2017.11.003>.
- (27) Zhu, Y.; Gao, C.; Liu, X.; Shen, J. Surface Modification of Polycaprolactone Membrane via Aminolysis and Biomacromolecule Immobilization for Promoting Cytocompatibility

- of Human Endothelial Cells. *Biomacromolecules* **2002**, *3* (6), 1312–1319. <https://doi.org/10.1021/bm020074y>.
- (28) Fabbri, P.; Messori, M. 5 - Surface Modification of Polymers: Chemical, Physical, and Biological Routes. In *Modification of Polymer Properties*; Jasso-Gastinel, C. F., Kenny, J. M., Eds.; William Andrew Publishing, 2017; pp 109–130. <https://doi.org/10.1016/B978-0-323-44353-1.00005-1>.
- (29) Stryczewska, H. D. Supply Systems of Non-Thermal Plasma Reactors. Construction Review with Examples of Applications. *Applied Sciences* **2020**, *10* (9), 3242. <https://doi.org/10.3390/app10093242>.
- (30) Xiang, Q.; Liu, X.; Li, J.; Ding, T.; Zhang, H.; Zhang, X.; Bai, Y. Influences of Cold Atmospheric Plasma on Microbial Safety, Physicochemical and Sensorial Qualities of Meat Products. *J Food Sci Technol* **2018**, *55* (3), 846–857. <https://doi.org/10.1007/s13197-017-3020-y>.
- (31) Sakudo, A.; Yagyu, Y.; Onodera, T. Disinfection and Sterilization Using Plasma Technology: Fundamentals and Future Perspectives for Biological Applications. *International Journal of Molecular Sciences* **2019**, *20* (20), 5216. <https://doi.org/10.3390/ijms20205216>.
- (32) Napartovich, A. P. Overview of Atmospheric Pressure Discharges Producing Nonthermal Plasma. *Plasmas and Polymers* **2001**, *6* (1), 1–14. <https://doi.org/10.1023/A:1011313322430>.
- (33) Domonkos, M.; Tichá, P.; Trejbal, J.; Demo, P. Applications of Cold Atmospheric Pressure Plasma Technology in Medicine, Agriculture and Food Industry. *Applied Sciences* **2021**, *11* (11), 4809. <https://doi.org/10.3390/app11114809>.
- (34) Peng, H. Y.; Devarajan, M.; Lee, T. T.; Lacey, D. Comparison of Radio Frequency and Microwave Plasma Treatments on LED Chip Bond Pad for Wire Bond Application. *IEEE Transactions on Components, Packaging and Manufacturing Technology* **2015**, *5* (4), 562–569. <https://doi.org/10.1109/TCPMT.2015.2406876>.
- (35) Singh, M.; Vajpayee, M.; Ledwani, L. Eco-Friendly Surface Modification and Nanofinishing of Textile Polymers to Enhance Functionalisation. In *Nanotechnology for Energy and Environmental Engineering*; Ledwani, L., Sangwai, J. S., Eds.; Green Energy and Technology; Springer International Publishing: Cham, 2020; pp 529–559. https://doi.org/10.1007/978-3-030-33774-2_23.
- (36) Nageswaran, G.; Jothi, L.; Jagannathan, S. Chapter 4 - Plasma Assisted Polymer Modifications. In *Non-Thermal Plasma Technology for Polymeric Materials*; Thomas, S., Mozetič, M., Cvelbar, U., Špatenka, P., K.m., P., Eds.; Elsevier, 2019; pp 95–127. <https://doi.org/10.1016/B978-0-12-813152-7.00004-4>.
- (37) Sofi, H. S.; Ashraf, R.; Khan, A. H.; Beigh, M. A.; Majeed, S.; Sheikh, F. A. Reconstructing Nanofibers from Natural Polymers Using Surface Functionalization Approaches for Applications in Tissue Engineering, Drug Delivery and Biosensing Devices. *Materials Science and Engineering: C* **2019**, *94*, 1102–1124. <https://doi.org/10.1016/j.msec.2018.10.069>.
- (38) Ivanovska, A.; Milošević, M.; Obradović, B.; Svirčev, Z.; Kostić, M. Plasma Treatment as a Sustainable Method for Enhancing the Wettability of Jute Fabrics. *Sustainability* **2023**, *15* (3), 2125. <https://doi.org/10.3390/su15032125>.
- (39) Vandenbossche, M.; Hegemann, D. Recent Approaches to Reduce Aging Phenomena in Oxygen- and Nitrogen-Containing Plasma Polymer Films: An Overview. *Current*

- Opinion in Solid State and Materials Science* **2018**, 22 (1), 26–38. <https://doi.org/10.1016/j.cossms.2018.01.001>.
- (40) Pérez-Calixto, M.; González-Pérez, G.; Dionisio, N.; Bucio, E.; Burillo, G.; García-Uriostegui, L. Surface Functionalization of Polypropylene and Polyethylene Films with Allylamine by γ Radiation. *MRS Communications* **2019**, 9 (1), 264–269. <https://doi.org/10.1557/mrc.2018.213>.
- (41) Bonferoni, M. C.; Caramella, C.; Catenacci, L.; Conti, B.; Dorati, R.; Ferrari, F.; Genta, I.; Modena, T.; Perteghella, S.; Rossi, S.; Sandri, G.; Sorrenti, M.; Torre, M. L.; Tripodo, G. Biomaterials for Soft Tissue Repair and Regeneration: A Focus on Italian Research in the Field. *Pharmaceutics* **2021**, 13 (9), 1341. <https://doi.org/10.3390/pharmaceutics13091341>.
- (42) Zare, M.; Ghomi, E. R.; Venkatraman, P. D.; Ramakrishna, S. Silicone-Based Biomaterials for Biomedical Applications: Antimicrobial Strategies and 3D Printing Technologies. *Journal of Applied Polymer Science* **2021**, 138 (38), 50969. <https://doi.org/10.1002/app.50969>.
- (43) Xing, H.; Lee, H.; Luo, L.; Kyriakides, T. R. Extracellular Matrix-Derived Biomaterials in Engineering Cell Function. *Biotechnol Adv* **2020**, 42, 107421. <https://doi.org/10.1016/j.biotechadv.2019.107421>.
- (44) Muncie, J. M.; Weaver, V. M. Chapter One - The Physical and Biochemical Properties of the Extracellular Matrix Regulate Cell Fate. In *Current Topics in Developmental Biology*; Litscher, E. S., Wassarman, P. M., Eds.; Extracellular Matrix and Egg Coats; Academic Press, 2018; Vol. 130, pp 1–37. <https://doi.org/10.1016/bs.ctdb.2018.02.002>.
- (45) Sotiri, I.; Robichaud, M.; Lee, D.; Braune, S.; Gorbet, M.; Ratner, B. D.; Brash, J. L.; Latour, R. A.; Reviakine, I. BloodSurf 2017: News from the Blood-Biomaterial Frontier. *Acta Biomaterialia* **2019**, 87, 55–60. <https://doi.org/10.1016/j.actbio.2019.01.032>.
- (46) Hu, W.-J.; Eaton, J. W.; Ugarova, T. P.; Tang, L. Molecular Basis of Biomaterial-Mediated Foreign Body Reactions. *Blood* **2001**, 98 (4), 1231–1238. <https://doi.org/10.1182/blood.V98.4.1231>.
- (47) Ozaltin, K.; Lehocký, M.; Kuceková, Z.; Humpolíček, P.; Sáha, P. A Novel Multistep Method for Chondroitin Sulphate Immobilization and Its Interaction with Fibroblast Cells. *Materials Science and Engineering: C* **2017**, 70, 94–100. <https://doi.org/10.1016/j.msec.2016.08.065>.
- (48) Zhao, W.; Ji, X.; Zhang, F.; Li, L.; Ma, L. Embryonic Stem Cell Markers. *Molecules* **2012**, 17 (6), 6196–6246. <https://doi.org/10.3390/molecules17066196>.
- (49) Humpolíček, P.; Kašpárková, V.; Pacherník, J.; Stejskal, J.; Bober, P.; Capáková, Z.; Radaszkiewicz, K. A.; Junkar, I.; Lehocký, M. The Biocompatibility of Polyaniline and Polypyrrole: A Comparative Study of Their Cytotoxicity, Embryotoxicity and Impurity Profile. *Materials Science and Engineering: C* **2018**, 91, 303–310. <https://doi.org/10.1016/j.msec.2018.05.037>.
- (50) Vroman, L. When Blood Is Touched. *Materials* **2009**, 2 (4), 1547–1557. <https://doi.org/10.3390/ma2041547>.
- (51) Dodo, C. G.; Senna, P. M.; Custodio, W.; Paes Leme, A. F.; Del Bel Cury, A. A. Proteome Analysis of the Plasma Protein Layer Adsorbed to a Rough Titanium Surface. *Biofouling* **2013**, 29 (5), 549–557. <https://doi.org/10.1080/08927014.2013.787416>.
- (52) Norde, W.; Lyklema, J. Why Proteins Prefer Interfaces. *Journal of Biomaterials Science, Polymer Edition* **1991**, 2 (3), 183–202. <https://doi.org/10.1080/09205063.1991.9756659>.

- (53) Vogler, E. A.; Graper, J. C.; Harper, G. R.; Sugg, H. W.; Lander, L. M.; Brittain, W. J. Contact Activation of the Plasma Coagulation Cascade. I. Procoagulant Surface Chemistry and Energy. *Journal of Biomedical Materials Research* **1995**, *29* (8), 1005–1016. <https://doi.org/10.1002/jbm.820290813>.
- (54) Simberg, D.; Zhang, W.-M.; Merkulov, S.; McCrae, K.; Park, J.-H.; Sailor, M. J.; Ruoslahti, E. Contact Activation of Kallikrein–Kinin System by Superparamagnetic Iron Oxide Nanoparticles in Vitro and in Vivo. *Journal of Controlled Release* **2009**, *140* (3), 301–305. <https://doi.org/10.1016/j.jconrel.2009.05.035>.
- (55) van der Poll, T. Tissue Factor as an Initiator of Coagulation and Inflammation in the Lung. *Critical Care* **2008**, *12* (6), S3. <https://doi.org/10.1186/cc7026>.
- (56) Gorbet, M. B.; Sefton, M. V. Biomaterial-Associated Thrombosis: Roles of Coagulation Factors, Complement, Platelets and Leukocytes. *Biomaterials* **2004**, *25* (26), 5681–5703. <https://doi.org/10.1016/j.biomaterials.2004.01.023>.
- (57) Palta, S.; Saroa, R.; Palta, A. Overview of the Coagulation System. *Indian J Anaesth* **2014**, *58* (5), 515–523. <https://doi.org/10.4103/0019-5049.144643>.
- (58) Greinacher, A.; Bakchoul, T.; Cuker, A.; Warkentin, T. (Ted) E. Heparin-Induced Thrombocytopenia. In *Platelets in Thrombotic and Non-Thrombotic Disorders: Pathophysiology, Pharmacology and Therapeutics: an Update*; Gresele, P., Kleiman, N. S., Lopez, J. A., Page, C. P., Eds.; Springer International Publishing: Cham, 2017; pp 789–811. https://doi.org/10.1007/978-3-319-47462-5_53.
- (59) Church, F. C.; Meade, J. B.; Treanor, R. E.; Whinna, H. C. Antithrombin Activity of Fucoidan: The Interaction of Fucoidan with Heparin Cofactor II, Antithrombin III, and Thrombin. *Journal of Biological Chemistry* **1989**, *264* (6), 3618–3623. [https://doi.org/10.1016/S0021-9258\(18\)94111-6](https://doi.org/10.1016/S0021-9258(18)94111-6).
- (60) Kuchinka, J.; Willems, C.; Telyshev, D. V.; Groth, T. Control of Blood Coagulation by Hemocompatible Material Surfaces—A Review. *Bioengineering* **2021**, *8* (12), 215. <https://doi.org/10.3390/bioengineering8120215>.
- (61) Ferraro, A. S.; Ronci, C.; Lanti, A.; Chiru, O. M.; Papa, A.; Insalaco, D.; Marconi, G.; Pattofatto, F.; Docimo, F.; De Masi, A.; Marino, D.; Ippolito, M.; Cipriani, C.; Guiducci, G.; Adorno, G. P28 - Antimicrobial Properties of Platelet Rich Plasma. *Transfusion and Apheresis Science* **2014**, *50*, S19–S20. [https://doi.org/10.1016/S1473-0502\(14\)50045-6](https://doi.org/10.1016/S1473-0502(14)50045-6).
- (62) Lee, Y.-E.; Kim, H.; Seo, C.; Park, T.; Lee, K. B.; Yoo, S.-Y.; Hong, S.-C.; Kim, J. T.; Lee, J. Marine Polysaccharides: Therapeutic Efficacy and Biomedical Applications. *Arch. Pharm. Res.* **2017**, *40* (9), 1006–1020. <https://doi.org/10.1007/s12272-017-0958-2>.
- (63) Smit, A. J. Medicinal and Pharmaceutical Uses of Seaweed Natural Products: A Review. *Journal of Applied Phycology* **2004**, *16* (4), 245–262. <https://doi.org/10.1023/B:JAPH.0000047783.36600.ef>.
- (64) Kim, J. M.; Bae, I.-H.; Lim, K. S.; Park, J.-K.; Park, D. S.; Lee, S.-Y.; Jang, E.-J.; Ji, M. S.; Sim, D. S.; Hong, Y. J.; Ahn, Y.; Park, J. C.; Cho, J. G.; Kang, J. C.; Kim, I.-S.; Jeong, M. H. A Method for Coating Fucoidan onto Bare Metal Stent and in Vivo Evaluation. *Progress in Organic Coatings* **2015**, *78*, 348–356. <https://doi.org/10.1016/j.porgcoat.2014.07.013>.
- (65) Morelli, A.; Puppi, D.; Chiellini, F. Chapter 16 - Perspectives on Biomedical Applications of Ulvan. In *Seaweed Polysaccharides*; Venkatesan, J., Anil, S., Kim, S.-K., Eds.; Elsevier, 2017; pp 305–330. <https://doi.org/10.1016/B978-0-12-809816-5.00016-5>.

- (66) Kersen, P.; Paalme, T.; Pajusalu, L.; Martin, G. Biotechnological Applications of the Red Alga *Furcellaria Lumbricalis* and Its Cultivation Potential in the Baltic Sea. *Botanica Marina* **2017**, *60* (2), 207–218. <https://doi.org/10.1515/bot-2016-0062>.
- (67) Weinberger, F.; Paalme, T.; Wikström, S. A. Seaweed Resources of the Baltic Sea, Kattegat and German and Danish North Sea Coasts. *Botanica Marina* **2020**, *63* (1), 61–72. <https://doi.org/10.1515/bot-2019-0019>.
- (68) Yang, B.; Yu, G.; Zhao, X.; Ren, W.; Jiao, G.; Fang, L.; Wang, Y.; Du, G.; Tiller, C.; Girouard, G.; Barrow, C. J.; Ewart, H. S.; Zhang, J. Structural Characterisation and Bioactivities of Hybrid Carrageenan-like Sulphated Galactan from Red Alga *Furcellaria Lumbricalis*. *Food Chemistry* **2011**, *124* (1), 50–57. <https://doi.org/10.1016/j.foodchem.2010.05.102>.
- (69) Tuvikene, R.; Truus, K.; Robal, M.; Volobujeva, O.; Mellikov, E.; Pehk, T.; Kollist, A.; Kailas, T.; Vaher, M. The Extraction, Structure, and Gelling Properties of Hybrid Galactan from the Red Alga *Furcellaria Lumbricalis* (Baltic Sea, Estonia). *Journal of Applied Phycology* **2010**, *22* (1), 51–63. <https://doi.org/10.1007/s10811-009-9425-x>.
- (70) Imeson, A. P. 7 - Carrageenan and Furcellaran. In *Handbook of Hydrocolloids (Second Edition)*; Phillips, G. O., Williams, P. A., Eds.; Woodhead Publishing Series in Food Science, Technology and Nutrition; Woodhead Publishing, 2009; pp 164–185. <https://doi.org/10.1533/9781845695873.164>.
- (71) Laos, K.; Ring, S. G. Note: Characterisation of Furcellaran Samples from Estonian *Furcellaria Lumbricalis* (Rhodophyta). *Journal of Applied Phycology* **2005**, *17* (5), 461–464. <https://doi.org/10.1007/s10811-005-1635-2>.
- (72) Kůrová, V.; Salek, R. N.; Černíková, M.; Lorencová, E.; Zalešáková, L.; Buňka, F. Furcellaran as a Substitute for Emulsifying Salts in Processed Cheese Spread and the Resultant Storage Changes. *International Journal of Dairy Technology* **2022**, *75* (3), 679–689. <https://doi.org/10.1111/1471-0307.12871>.
- (73) Marangoni Júnior, L.; Vieira, R. P.; Jamróz, E.; Anjos, C. A. R. Furcellaran: An Innovative Biopolymer in the Production of Films and Coatings. *Carbohydrate Polymers* **2021**, *252*, 117221. <https://doi.org/10.1016/j.carbpol.2020.117221>.
- (74) Milosavljevic, V.; Jamroz, E.; Gagic, M.; Haddad, Y.; Michalkova, H.; Balkova, R.; Tesarova, B.; Moulick, A.; Heger, Z.; Richtera, L.; Kopel, P.; Adam, V. Encapsulation of Doxorubicin in Furcellaran/Chitosan Nanocapsules by Layer-by-Layer Technique for Selectively Controlled Drug Delivery. *Biomacromolecules* **2020**, *21* (2), 418–434. <https://doi.org/10.1021/acs.biomac.9b01175>.
- (75) Jasińska, J. M.; Kamińska, I.; Chmiel, M. J.; Jamróz, E. Biological Potential of Polysaccharides Extracted from Nostoc Colonies for Film Production – Physical and Biological Properties. *Biotechnology Journal* *n/a* (n/a), 2200455. <https://doi.org/10.1002/biot.202200455>.
- (76) Raveendran, S.; Yoshida, Y.; Maekawa, T.; Kumar, D. S. Pharmaceutically Versatile Sulfated Polysaccharide Based Bionano Platforms. *Nanomedicine: Nanotechnology, Biology and Medicine* **2013**, *9* (5), 605–626. <https://doi.org/10.1016/j.nano.2012.12.006>.
- (77) Cunha, L.; Grenha, A. Sulfated Seaweed Polysaccharides as Multifunctional Materials in Drug Delivery Applications. *Mar Drugs* **2016**, *14* (3), 42. <https://doi.org/10.3390/md14030042>.
- (78) Zhao, T.; Yang, M.; Ma, L.; Liu, X.; Ding, Q.; Chai, G.; Lu, Y.; Wei, H.; Zhang, S.; Ding, C. Structural Modification and Biological Activity of Polysaccharides. *Molecules* **2023**, *28* (14), 5416. <https://doi.org/10.3390/molecules28145416>.

- (79) Benedetti, A. M.; Gill, D. M.; Tsang, C. W.; Jones, A. M. Chemical Methods for N- and O-Sulfation of Small Molecules, Amino Acids and Peptides. *ChemBioChem* **2020**, *21* (7), 938–942. <https://doi.org/10.1002/cbic.201900673>.
- (80) Dantas-Santos, N.; Gomes, D. L.; Costa, L. S.; Cordeiro, S. L.; Costa, M. S. S. P.; Trindade, E. S.; Franco, C. R. C.; Scortecchi, K. C.; Leite, E. L.; Rocha, H. A. O. Freshwater Plants Synthesize Sulfated Polysaccharides: Heterogalactans from Water Hyacinth (*Eichhornia Crassipes*). *International Journal of Molecular Sciences* **2012**, *13* (1), 961–976. <https://doi.org/10.3390/ijms13010961>.
- (81) Chagas, F. D. da S.; Lima, G. C.; dos Santos, V. I. N.; Costa, L. E. C.; de Sousa, W. M.; Sombra, V. G.; de Araújo, D. F.; Barros, F. C. N.; Marinho-Soriano, E.; de Andrade Feitosa, J. P.; de Paula, R. C. M.; Pereira, M. G.; Freitas, A. L. P. Sulfated Polysaccharide from the Red Algae *Gelidiella Acerosa*: Anticoagulant, Antiplatelet and Antithrombotic Effects. *International Journal of Biological Macromolecules* **2020**, *159*, 415–421. <https://doi.org/10.1016/j.ijbiomac.2020.05.012>.
- (82) Li, S.; Dai, S.; Shah, N. P. Sulfonation and Antioxidative Evaluation of Polysaccharides from Pleurotus Mushroom and Streptococcus Thermophilus Bacteria: A Review. *Comprehensive Reviews in Food Science and Food Safety* **2017**, *16* (2), 282–294. <https://doi.org/10.1111/1541-4337.12252>.
- (83) Chahidedgumjorn, A.; Toyoda, H.; Woo, E. R.; Lee, K. B.; Kim, Y. S.; Toida, T.; Imanari, T. Effect of (1→3)- and (1→4)-Linkages of Fully Sulfated Polysaccharides on Their Anticoagulant Activity. *Carbohydrate Research* **2002**, *337* (10), 925–933. [https://doi.org/10.1016/S0008-6215\(02\)00078-2](https://doi.org/10.1016/S0008-6215(02)00078-2).
- (84) Groult, H.; Cousin, R.; Chot-Plassot, C.; Maura, M.; Bridiau, N.; Piot, J.-M.; Maugard, T.; Fruitier-Arnaudin, I. λ -Carrageenan Oligosaccharides of Distinct Anti-Heparanase and Anticoagulant Activities Inhibit MDA-MB-231 Breast Cancer Cell Migration. *Marine Drugs* **2019**, *17* (3), 140. <https://doi.org/10.3390/md17030140>.
- (85) Al-Horani, R. A.; Desai, U. R. Chemical Sulfation of Small Molecules – Advances and Challenges. *Tetrahedron* **2010**, *66* (16), 2907–2918. <https://doi.org/10.1016/j.tet.2010.02.015>.
- (86) Becher, J.; Möller, S.; Weiss, D.; Schiller, J.; Schnabelrauch, M. Synthesis of New Regioselectively Sulfated Hyaluronans for Biomedical Application. *Macromolecular Symposia* **2010**, *296* (1), 446–452. <https://doi.org/10.1002/masy.201051060>.
- (87) Papy-Garcia, D.; Barbier-Chassefière, V.; Rouet, V.; Kerros, M.-E.; Klochendler, C.; Tournaire, M.-C.; Barritault, D.; Caruelle, J.-P.; Petit, E. Nondegradative Sulfation of Polysaccharides. Synthesis and Structure Characterization of Biologically Active Heparan Sulfate Mimetics. *Macromolecules* **2005**, *38* (11), 4647–4654. <https://doi.org/10.1021/ma048485p>.
- (88) Manik, E. R.; Kaban, J. Synthesis of Sulfated Chitosan Through Sulfation Reaction of Chitosan with Chlorosulfonic Acid in N, N-Dimethylformamide, and Antibacterial Activity Test. *Journal of Chemical Natural Resources* **2022**, *4* (1), 1–8. <https://doi.org/10.32734/jcnar.v4i1.9353>.
- (89) Arlov, Ø.; Rüttsche, D.; Asadi Korayem, M.; Öztürk, E.; Zenobi-Wong, M. Engineered Sulfated Polysaccharides for Biomedical Applications. *Advanced Functional Materials* **2021**, *31* (19), 2010732. <https://doi.org/10.1002/adfm.202010732>.
- (90) Padeste, C.; Farquet, P.; Potzner, C.; Solak, H. H. Nanostructured Bio-Functional Polymer Brushes. *Journal of Biomaterials Science, Polymer Edition* **2012**. <https://doi.org/10.1163/156856206778667505>.

- (91) Zhou, T.; Zhu, Y.; Li, X.; Liu, X.; Yeung, K. W. K.; Wu, S.; Wang, X.; Cui, Z.; Yang, X.; Chu, P. K. Surface Functionalization of Biomaterials by Radical Polymerization. *Progress in Materials Science* **2016**, *83*, 191–235. <https://doi.org/10.1016/j.pmatsci.2016.04.005>.
- (92) Bílek, F.; Křížová, T.; Lehocký, M. Preparation of Active Antibacterial LDPE Surface through Multistep Physicochemical Approach: I. Allylamine Grafting, Attachment of Antibacterial Agent and Antibacterial Activity Assessment. *Colloids and Surfaces B: Biointerfaces* **2011**, *88* (1), 440–447. <https://doi.org/10.1016/j.colsurfb.2011.07.027>.
- (93) Aziz, G.; De Geyter, N.; Declercq, H.; Cornelissen, R.; Morent, R. Incorporation of Amine Moieties onto Ultra-High Molecular Weight Polyethylene (UHMWPE) Surface via Plasma and UV Polymerization of Allylamine. *Surface and Coatings Technology* **2015**, *271*, 39–47. <https://doi.org/10.1016/j.surcoat.2015.01.027>.
- (94) Tran, C. T. H.; Kondyurin, A.; Chrzanowski, W.; Bilek, M. M. M.; McKenzie, D. R. Increasing Binding Density of Yeast Cells by Control of Surface Charge with Allylamine Grafting to Ion Modified Polymer Surfaces. *Colloids and Surfaces B: Biointerfaces* **2014**, *122*, 537–544. <https://doi.org/10.1016/j.colsurfb.2014.07.026>.
- (95) Wang, Y.; Shen, Y.; Pei, X.; Zhang, W.; Wei, Y.; Yang, C. In Situ Synthesis of Polystyrene/SiO₂ Hybrid Composites via a “Grafting Through” Strategy Based on Nitroxide-Mediated Radical Polymerisation. *Polymers and Polymer Composites* **2008**, *16* (9), 621–626. <https://doi.org/10.1177/096739110801600906>.
- (96) Kyzioł, A.; Kyzioł, K. Chapter 4 - Surface Functionalization With Biopolymers via Plasma-Assisted Surface Grafting and Plasma-Induced Graft Polymerization—Materials for Biomedical Applications. In *Biopolymer Grafting*; Thakur, V. K., Ed.; Elsevier, 2018; pp 115–151. <https://doi.org/10.1016/B978-0-12-810462-0.00004-1>.
- (97) del Hoyo-Gallego, S.; Pérez-Álvarez, L.; Gómez-Galván, F.; Lizundia, E.; Kuritka, I.; Sedlarik, V.; Laza, J. M.; Vila-Vilela, J. L. Construction of Antibacterial Poly(Ethylene Terephthalate) Films via Layer by Layer Assembly of Chitosan and Hyaluronic Acid. *Carbohydrate Polymers* **2016**, *143*, 35–43. <https://doi.org/10.1016/j.carbpol.2016.02.008>.
- (98) Yang, J.; Bei, J.; Wang, S. Enhanced Cell Affinity of Poly (d,l-Lactide) by Combining Plasma Treatment with Collagen Anchorage. *Biomaterials* **2002**, *23* (12), 2607–2614. [https://doi.org/10.1016/S0142-9612\(01\)00400-8](https://doi.org/10.1016/S0142-9612(01)00400-8).
- (99) Liu, Y.; He, T.; Gao, C. Surface Modification of Poly(Ethylene Terephthalate) via Hydrolysis and Layer-by-Layer Assembly of Chitosan and Chondroitin Sulfate to Construct Cytocompatible Layer for Human Endothelial Cells. *Colloids and Surfaces B: Biointerfaces* **2005**, *46* (2), 117–126. <https://doi.org/10.1016/j.colsurfb.2005.09.005>.
- (100) Nguyen, H. H.; Kim, M. An Overview of Techniques in Enzyme Immobilization. *Applied Science and Convergence Technology* **2017**, *26* (6), 157–163. <https://doi.org/10.5757/ASCT.2017.26.6.157>.
- (101) Niemczyk-Soczynska, B.; Gradys, A.; Sajkiewicz, P. Hydrophilic Surface Functionalization of Electrospun Nanofibrous Scaffolds in Tissue Engineering. *Polymers* **2020**, *12* (11), 2636. <https://doi.org/10.3390/polym12112636>.
- (102) Štěpánková, K.; Ozaltin, K.; Pelková, J.; Pištěková, H.; Karakurt, I.; Káčerová, S.; Lehocký, M.; Humpolicek, P.; Vesel, A.; Mozetic, M. Furcellaran Surface Deposition and Its Potential in Biomedical Applications. *International Journal of Molecular Sciences* **2022**, *23* (13), 7439. <https://doi.org/10.3390/ijms23137439>.

- (103) Yamashita, S.; Sugita-Konishi, Y.; Shimizu, M. In Vitro Bacteriostatic Effects of Dietary Polysaccharides. *Food Science and Technology Research* **2001**, *7* (3), 262–264. <https://doi.org/10.3136/fstr.7.262>.
- (104) Bajpai, S. K.; Daheriya, P. Kappa-Carrageenan/PVA Films with Antibacterial Properties: Part 1. Optimization of Preparation Conditions and Preliminary Drug Release Studies. *Journal of Macromolecular Science, Part A* **2014**, *51* (4), 286–295. <https://doi.org/10.1080/10601325.2014.882687>.
- (105) Ozaltin, K.; Lehocký, M.; Humpolíček, P.; Pelková, J.; Sába, P. A New Route of Fucoidan Immobilization on Low Density Polyethylene and Its Blood Compatibility and Anticoagulation Activity. *IJMS* **2016**, *17* (6), 908. <https://doi.org/10.3390/ijms17060908>.
- (106) Wei, J.; Yoshinari, M.; Takemoto, S.; Hattori, M.; Kawada, E.; Liu, B.; Oda, Y. Adhesion of Mouse Fibroblasts on Hexamethyldisiloxane Surfaces with Wide Range of Wettability. *J Biomed Mater Res B Appl Biomater* **2007**, *81* (1), 66–75. <https://doi.org/10.1002/jbm.b.30638>.
- (107) Cvelbar, U.; Junkar, I.; Modic, M. Hemocompatible Poly(Ethylene Terephthalate) Polymer Modified via Reactive Plasma Treatment. *Jpn. J. Appl. Phys.* **2011**, *50* (8S1), 08JF02. <https://doi.org/10.1143/JJAP.50.08JF02>.
- (108) Ko, J.-Y.; Lee, J.-H.; Kim, H.-S.; Kim, H.-H.; Jeon, Y.-J. Cell proliferation effect of brown marine algae extracts on Mouse Fibroblast. *Journal of Marine Bioscience and Biotechnology* **2015**, *7* (1), 28–34. <https://doi.org/10.15433/ksmb.2015.7.1.028>.
- (109) Ozaltin, K.; Vargun, E.; Di Martino, A.; Capakova, Z.; Lehocky, M.; Humpolicek, P.; Kazantseva, N.; Saha, P. Cell Response to PLA Scaffolds Functionalized with Various Seaweed Polysaccharides. *International Journal of Polymeric Materials and Polymeric Biomaterials* **2022**, *71* (2), 79–86. <https://doi.org/10.1080/00914037.2020.1798443>.
- (110) Kishimoto, T. K.; Viswanathan, K.; Ganguly, T.; Elankumaran, S.; Smith, S.; Pelzer, K.; Lansing, J. C.; Sriranganathan, N.; Zhao, G.; Galcheva-Gargova, Z.; Al-Hakim, A.; Bailey, G. S.; Fraser, B.; Roy, S.; Rogers-Cotrone, T.; Buhse, L.; Whary, M.; Fox, J.; Nasr, M.; Dal Pan, G. J.; Shriver, Z.; Langer, R. S.; Venkataraman, G.; Austen, K. F.; Woodcock, J.; Sasisekharan, R. Contaminated Heparin Associated with Adverse Clinical Events and Activation of the Contact System. *New England Journal of Medicine* **2008**, *358* (23), 2457–2467. <https://doi.org/10.1056/NEJMoa0803200>.
- (111) Kazachenko, A. S.; Vasilieva, N. Yu.; Fetisova, O. Yu.; Sychev, V. V.; Elsufov, E. V.; Malyar, Y. N.; Issaoui, N.; Miroshnikova, A. V.; Borovkova, V. S.; Kazachenko, A. S.; Berezhnaya, Y. D.; Skripnikov, A. M.; Zimonin, D. V.; Ionin, V. A. New Reactions of Betulin with Sulfamic Acid and Ammonium Sulfamate in the Presence of Solid Catalysts. *Biomass Conv. Bioref.* **2022**. <https://doi.org/10.1007/s13399-022-02587-x>.
- (112) Silva, F. R. F.; Dore, C. M. P. G.; Marques, C. T.; Nascimento, M. S.; Benevides, N. M. B.; Rocha, H. A. O.; Chavante, S. F.; Leite, E. L. Anticoagulant Activity, Paw Edema and Pleurisy Induced Carrageenan: Action of Major Types of Commercial Carrageenans. *Carbohydrate Polymers* **2010**, *79* (1), 26–33. <https://doi.org/10.1016/j.carbpol.2009.07.010>.
- (113) Li, H.; Wang, X.; Xiong, Q.; Yu, Y.; Peng, L. Sulfated Modification, Characterization, and Potential Bioactivities of Polysaccharide from the Fruiting Bodies of *Russula Virescens*. *International Journal of Biological Macromolecules* **2020**, *154*, 1438–1447. <https://doi.org/10.1016/j.ijbiomac.2019.11.025>.

- (114) Xie, X.-T.; Zhang, X.; Liu, Y.; Chen, X.-Q.; Cheong, K.-L. Quantification of 3,6-Anhydro-Galactose in Red Seaweed Polysaccharides and Their Potential Skin-Whitening Activity. *3 Biotech* **2020**, *10* (4), 189. <https://doi.org/10.1007/s13205-020-02175-8>.
- (115) Prado-Fernández, J.; Rodríguez-Vázquez, J. A.; Tojo, E.; Andrade, J. M. Quantitation of κ -, ι - and λ -Carrageenans by Mid-Infrared Spectroscopy and PLS Regression. *Analytica Chimica Acta* **2003**, *480* (1), 23–37. [https://doi.org/10.1016/S0003-2670\(02\)01592-1](https://doi.org/10.1016/S0003-2670(02)01592-1).
- (116) Yang, J.; Du, Y.; Wen, Y.; Li, T.; Hu, L. Sulfation of Chinese Lacquer Polysaccharides in Different Solvents. *Carbohydrate Polymers* **2003**, *52* (4), 397–403. [https://doi.org/10.1016/S0144-8617\(02\)00330-2](https://doi.org/10.1016/S0144-8617(02)00330-2).
- (117) Jamalzadeh, L.; Ghafoori, H.; Sariri, R.; Rabuti, H.; Nasirzade, J.; Hasani, H.; Aghamaali, M. R. Cytotoxic Effects of Some Common Organic Solvents on MCF-7, RAW-264.7 and Human Umbilical Vein Endothelial Cells. *Avicenna J Med Biochem* **2016**, *4* (1), 10–33453. <https://doi.org/10.17795/ajmb-33453>.
- (118) Liang, W.; Mao, X.; Peng, X.; Tang, S. Effects of Sulfate Group in Red Seaweed Polysaccharides on Anticoagulant Activity and Cytotoxicity. *Carbohydrate Polymers* **2014**, *101*, 776–785. <https://doi.org/10.1016/j.carbpol.2013.10.010>.
- (119) Fonseca, R. J. C.; Oliveira, S.-N. M. C. G.; Melo, F. R.; Pereira, M. G.; Benevides, N. M. B.; Mourão, P. A. S. Slight Differences in Sulfation of Algal Galactans Account for Differences in Their Anticoagulant and Venous Antithrombotic Activities. *Thromb Haemost* **2008**, *99* (3), 539–545. <https://doi.org/10.1160/TH07-10-0603>.
- (120) Saluri, K.; Tuvikene, R. Anticoagulant and Antioxidant Activity of Lambda- and Theta-Carrageenans of Different Molecular Weights. *Bioactive Carbohydrates and Dietary Fibre* **2020**, *24*, 100243. <https://doi.org/10.1016/j.bcdf.2020.100243>.
- (121) Leung, M. Y. K.; Liu, C.; Koon, J. C. M.; Fung, K. P. Polysaccharide Biological Response Modifiers. *Immunology Letters* **2006**, *105* (2), 101–114. <https://doi.org/10.1016/j.imlet.2006.01.009>.
- (122) Pomin, V. H.; Mourão, P. A. S. Specific Sulfation and Glycosylation—a Structural Combination for the Anticoagulation of Marine Carbohydrates. *Front Cell Infect Microbiol* **2014**, *4*, 33. <https://doi.org/10.3389/fcimb.2014.00033>.
- (123) Liang, W.; Mao, X.; Peng, X.; Tang, S. Effects of Sulfate Group in Red Seaweed Polysaccharides on Anticoagulant Activity and Cytotoxicity. *Carbohydrate Polymers* **2014**, *101*, 776–785. <https://doi.org/10.1016/j.carbpol.2013.10.010>.
- (124) Melo, F. R.; Pereira, M. S.; Foguel, D.; Mourão, P. A. S. Antithrombin-Mediated Anticoagulant Activity of Sulfated Polysaccharides: DIFFERENT MECHANISMS FOR HEPARIN AND SULFATED GALACTANS*. *Journal of Biological Chemistry* **2004**, *279* (20), 20824–20835. <https://doi.org/10.1074/jbc.M308688200>.
- (125) Lee, C. J.; Ansell, J. E. Direct Thrombin Inhibitors. *Br J Clin Pharmacol* **2011**, *72* (4), 581–592. <https://doi.org/10.1111/j.1365-2125.2011.03916.x>.

LIST OF FIGURES

| | |
|---|----|
| Figure 1 Plasma classification. Note: T_e = electron temperature, T_i = ion temperature, T_g = gas temperature ³⁰ | 12 |
| Figure 2 Plasma classification based on pressure ³⁰ | 12 |
| Figure 3 Morfology of A) fibroblasts NIH/3T3 and B) embryonic stem cells ES R1 line ^{47,49} | 14 |
| Figure 4 Discoid platelet (a), dendritic platelet (b) and spread platelet (c) photographed in the low-voltage, high-resolution SEM ⁶¹ | 16 |
| Figure 5 Furcellaran structure..... | 17 |
| Figure 6 The proposed mechanism involves the formation of a solvated, protonated DCC/H ₂ SO ₄ intermediate with a subsequent attack of the alcohol group on the sulfur atom, resulting in the production of dicyclohexylurea and the monosulfate ester ⁸⁵ | 19 |
| Figure 7 The suggested reaction mechanism furcellaran sulfation with chlorosulfonic acid and a dimethylformamide intermediate ⁸⁹ | 20 |
| Figure 8 An adsorptive immobilization of biomolecule with sulfate group(s) and positively charged nitrogen containing groups on the surface by Coulomb-type interactions and hydrogen bonding | 21 |
| Figure 9 Schematic representation of plasma postirradiation grafting of N-allylmethylamine onto a PET surface followed by immobilization of FUR or κ -CA polysaccharide ¹⁰² | 24 |
| Figure 10 SEM micrographs of (a) untreated PET, (b) PET_DC, (c) DC_MAAM, (d) MAAM_1000, (e) MAAM_8500, (f) MAAM_KAPA, (g) DC_1000, (h) DC_8500 and (i) DC_KAPA..... | 27 |
| Figure 11 Relative cell viability of cells incubated with PET films coated with furcellaran of different water gel strengths (1000, 8500) and κ -carrageenan tested on a mouse embryonic fibroblast cell line (NIH/3T3). | 30 |
| Figure 12 Cell viability in the ES R1 cell line with comparison of (A) reference (TPP) and PET; (B) TPP and PET coated with gelatine; (C) PET as a reference and samples; (D) PET and samples coated with gelatine.; * $p < 0.05$, ** $p < 0.01$, *** $p < 0.001$ | 31 |
| Figure 13 Mouse embryonic cells (Line R1) on A) PET uncoated with 0.1% gelatine and B) DC 8500 uncoated with 0.1% gelatine | 32 |
| Figure 14 Schematic representation of sulfation methods with targeted sulfate position. The structures do not reflect the strict composition of the sample..... | 34 |

Figure 15 Attenuated total reflectance (ATR)-FT-IR spectrum collected from the samples. Spectrum (a) is for FUR, spectrum (b) is for FUR_DMSO, spectrum (c) is for FUR_DMF, spectrum (d) is for FUR_HSO3CL and spectrum (e) is for FUR_DCC..... 37

Figure 16 XPS spectra: a) overlay of the high-resolution C 1s scans for furcellaran and its derivates. Inset displays the results of C 1s deconvolution for FUR sample, b) binding of sulfate for FUR_DMSO as representative sample..... 38

Figure 17 Relative cell viability values expressed as a percent of control (expanded polystyrene); * p < 0.05, ** p < 0.01, *** p < 0.001..... 39

Figure 18 Anticoagulation activity results; A) aPTT: activated partial thromboplastin time; B) TT: thrombin time; C) PT: prothrombin time. The significant differences compared to the control group (NS: negative control, saline solution) are designated as * p < 0.05; ** p < 0.01; *** p < 0.001. The clotting time of saline solution in the PT, APTT and TT assays was 13.5 s, 29.1 s, and 18.5 s, respectively. No coagulation response was observed for sodium heparin (positive control) across the range of concentrations tested. 40

Figure 19 Morphology of platelets a) untreated PET, b) FUR_HSO3CL c) untreated PET, d) FUR_HSO3CL, e) Air plasma treated PET_DC, f) FUR, g) FUR_DMSO, h) FUR_DMF, i) FUR_DCC. Two different magnifications are shown: 1000 × (a, b) and 3000 × (c–i)..... 41

LIST OF TABLES

Table 1 Contact angles (θ) (w: deionized water; d: diiodomethane; f: formamide) and surface free energy parameters of probe liquids used in the acid-base method (γ_g – total surface free energy, apolar γ_sLW , polar γ_sAB , Lewis acid γ_{s+} and base γ_s - components)..... 26

Table 2 Surface elemental composition (%) 27

Table 3 Anticoagulant activity expressed by clotting times 29

Table 4 Molecular weight and elemental composition and degree of sulfation of tested samples..... 36

LIST OF ABBREVIATIONS AND SYMBOLS

| | |
|---------------------|--|
| aPPT | Activated Partial Thromboplastin Time |
| ATR | Attenuated total reflectance |
| κ -CA | κ -Carrageenan |
| DC | Direct Current |
| DCC | N, N'-Dicyclohexylcarbodiimide |
| DMF | Dimethylformamide |
| DMSO | Dimethyl sulfoxide |
| DS | Degree of Substitution |
| EC | Embryonic cell |
| FT-IR | Fourier-Transform Infrared Spectroscopy |
| GPC | Gel Permeation Chromatography |
| HPLC | High-Performance Liquid Chromatography |
| HSO ₃ Cl | Chlorosulfonic acid |
| MAAM | N-allylmethylamine |
| MIC | Minimal Inhibitory Concentration |
| MTT | 3-(4,5-Dimethylthiazol-2-yl)-2,5-Diphenyltetrazolium Bromide |
| PET | Polyethylene terephthalate |
| PRP | Platelet-Rich Plasma |
| PT | Prothrombin Time |
| SEM | Scanning electron microscopy |
| SO ₃ ·Py | Sulfur trioxide pyridine complex |
| sccm | Standard cubic centimetre per minute |
| XPS | Photoelectron spectroscopy |
| θ | Contact angle |
| γ | Surface energy |

LIST OF PUBLICATIONS

Articles published in journals indexed on Web of Science

Botelho, A.; Penha, A.; Fraga, J.; Barros-Timmons, A.; Coelho, M. A.; Lehocky, M.; **Štěpánková, K.**; Amaral, P. Yarrowia Lipolytica Adhesion and Immobilization onto Residual Plastics. *Polymers* 2020, 12 (3), 649. <https://doi.org/10.3390/polym12030649>. (**ARTICLE I**)

Author contribution: Sample characterization – contact angle and surface energy.

Karakurt, I.; Ozaltin, K.; Vargun, E.; Kucerova, L.; Suly, P.; Harea, E.; Minařík, A.; **Štěpánková, K.**; Lehocky, M.; Humpolíček, P.; Vesel, A.; Mozetic, M. Controlled Release of Enrofloxacin by Vanillin-Crosslinked Chitosan-Polyvinyl Alcohol Blends. *Mater Sci Eng C Mater Biol Appl* 2021, 126, 112125. <https://doi.org/10.1016/j.msec.2021.112125>. (**ARTICLE II**)

Author contribution: Sample characterization – measurements of drug release profiles.

Štěpánková, K.; Ozaltin, K.; Pelková, J.; Pištěková, H.; Karakurt, I.; Káčerová, S.; Lehocky, M.; Humpolíček, P.; Vesel, A.; Mozetic, M. Furcellaran Surface Deposition and Its Potential in Biomedical Applications. *International Journal of Molecular Sciences* 2022, 23 (13), 7439. <https://doi.org/10.3390/ijms23137439>. (**ARTICLE III**)

Author contribution: Sample preparation including modification of substrates and deposition of polysaccharides onto films, characterization – contact angle and surface energy, antibacterial testing, taking part on the anticoagulation activity characterization. First draft writing and taking part on final manuscript edition.

Štěpánková, K., Ozaltin, K., Gorejova, R., Doudova, H., Domincová-Bergerová, E., Maskalova, I., Stupavska, M., Sřahel, P., Trunec, D., Pelková, J., Mozetic, M. and Lehocky, M., Sulfation of Furcellaran and its Effect on Hemocompatibility in vitro. *International Journal of Biological Macromolecules* 2024. 258, 128840. <https://doi.org/10.1016/j.ijbiomac.2023.128840>. (**ARTICLE IV**)

Author contribution: *Sample preparation including modification of substrates and deposition of polysaccharides onto films, characterization – contact angle and surface energy, FTIR and platelet adhesion testing First draft writing and taking part on final manuscript edition.*

Štěpánková, K., Ozaltin, K., Domincová-Bergerová, E., Mozetič, M., Vesel, A. and Lehocký, M., Carboxymethylated and Sulfated Furcellaran From *Furcellaria Lumbricalis* and Its Immobilization on PLA Scaffolds. *Polymers* (submitted) **(ARTICLE V)**

Author contribution: *Sample preparation including modification of substrates and deposition of polysaccharides onto films, characterization – contact angle, FTIR, SEM. First draft writing and taking part on final manuscript edition.*

CURRICULUM VITAE

Name: Kateřina ŠTĚPÁNKOVÁ
Date of birth: 11th May 1995
Nationality: Czech
Permanent address: Frýdek-Místek, 738 01 Czech Republic
E-mail: k1_stepankova@utb.cz

Education: **2019 – to date**
Doctoral degree
Centre of Polymer Systems,
Tomas Bata University in Zlin (Czech Republic)
Biomaterials and Biocomposites

2017 – 2019
Master's degree
Faculty of Technology,
Tomas Bata University in Zlin (Czech Republic)
Chemistry of food and bioactive compounds

2014 – 2017
Bachelor's degree
Faculty of Technology,
Tomas Bata University in Zlin (Czech Republic)
Chemistry and food technology

Education stays:**May 2022**

Pavol Josef Šafárik University in Košice – characterization of samples by platelet adhesion method and hemolysis, Košice, Slovakia

September-November 2022

University of Aveiro, traineeship – Preparation and characterization of gelatin capsules for controlled delivery of active species; Universidade de Aveiro, 3810-193 Aveiro, Portugal

Projects:**Internal funding**

- IGA/CPS/2020/001 – Biocompatibility and antimicrobial activity of materials
- IGA/CPS/2021/001 – Biocompatibility of materials
- IGA/CPS/2022/001 – Preparation of advanced biomaterials and their application
- IGA/CPS/2023/001 – Preparation of advanced biomaterials and their applications

Pedagogic activities

Participation on teaching in classes of “Introduction to materials for medicine and cosmetics”, TUTTTK / TP1UK (FT, UTB).

CONFERENCES ATTENDED

1. Lehocky M., Stepankova K.: Modification of polymer substrates for biomedical applications by multistep physico-chemical approach, Plastko, 2022, Zlín (Czech Republic)
2. Lehocky M., Stepankova K., Karakurt I., Ozaltin K. and Humpolicek P.: Surface deposition of polysaccharides on plasma treated polymer surfaces for biomedical applications, 94th IUUVISTA workshop of reliable sensing and control of reactive plasmas, 2022, Kranjska Gora (Slovenia) – invited lecture.
3. Lehocky M., Stepankova K., Mozetic, M.: Plasma assisted polymer biofunctionalization, 24th Symposium on Application of Plasma Processes and 13th EU-Japan Joint Symposium on Plasma Processing, 2023, Štrbské Pleso (Slovakia) – invited lecture.
4. Stepankova, K, Ozaltin, K., Gorejová, R., Pelková J., Lehocky M., The Impact of Furcellaran Sulfation on Blood Compatibility, ICAPT-8, 2023, Gozd Martuljek (Slovenia)
5. Stepankova, K, Ozaltin, K., Gorejová, R., Pelková J., Lehocky M., Furcellaran Sulfation for Improved Blood Compatibility, SPE MINITEC, 2023, Zlín (Czech Republic)

Ing. Kateřina Štěpánková, Ph.D.

Chemical Modification of Polysaccharides for Biomedical Applications

Chemická modifikace polysacharidů pro biomedicínské aplikace

Doctoral Thesis Summary

Published by: Tomas Bata University in Zlín

nám. T. G. Masaryka 5555, 760 01 Zlín

Edition: published electronically

Typesetting by: Ing. Kateřina Štěpánková, Ph.D.

This publication has not undergone any proofreading or editorial review.

Publication year: 2024

First Edition

ISBN 978-80-7678-240-2